PNAS

Supporting Information for

Divalent siRNAs are bioavailable in the lung and efficiently block SARS-CoV-2 infection.

Vignesh N. Hariharan[1#], Minwook Shin[1#], Ching-Wen Chang[2#], Daniel O'Reilly[1], Annabelle Biscans[1], Ken Yamada[1], Zhiru Guo[2], Mohan Somasundaran[3], Qi Tang[1], Kathryn Monopoli[1], Pranathi Meda Krishnamurthy[1], Gitali Devi[1], Nicholas McHugh[1], David A. Cooper[1], Dimas Echeverria[1], John Cruz[4], Io Long Chan[1], Ping Liu[2], Sun-Young Lim[2], Jill McConnell[5], Satya Prakash Singh[2], Samuel Hildebrand[1], Jacquelyn Sousa[1], Sarah M. Davis[1], Zachary Kennedy[1], Chantal Ferguson[1], Bruno M. D. C. Godinho[1], Yann Thillier[1], Jillian Caiazzi[1], Socheata Ly[1], Manish Muhuri[5,8], Karen Kelly[1], Fiachra Humphries[7], Alyssa Cousineau[6], Krishna Mohan Parsi[6], Qi Li[9], Yang Wang[9], René Maehr[6], Guangping Gao[5,8,10], Dmitry Korkin[11], William M. McDougall[5], Robert W. Finberg[2]†, Katherine A. Fitzgerald[7,10]*, Jennifer P. Wang[2]*, Jonathan K. Watts[1, 10]*, and Anastasia Khvorova[1]*

[1]RNA Therapeutics Institute, [2]Department of Medicine, [3]Department of Biochemistry and Molecular Biotechnology, [4]Department of Pathology, [5]Department of Microbiology and Physiological Systems, [6]Diabetes Center of Excellence and Program in Molecular Medicine, [7]Program in Innate Immunity, Division of Infectious Diseases and Immunology, Department of Medicine, [8]Horae Gene Therapy Center, [9]MassBiologics, [10]Li Weibo Institute for Rare Diseases Research, University of Massachusetts Chan Medical School; [11]Department of Computer Science, and Bioinformatics and Computational Biology Program, Worcester Polytechnic Institute; Worcester, USA.

*Corresponding authors. Email: kate.fitzgerald@umassmed.edu; jennifer.wang@umassmed.edu; jonathan.watts@umassmed.edu; anastasia.khvorova@umassmed.edu

#These authors contributed to the paper equally
†This paper is dedicated to the memory of Robert W. Finberg, a great physician-scientist and mentor whose contributions to the COVID-19 response are invaluable.

This PDF file includes:

Supplementary Methods
Figures S1 to S13
Supplemental Table 1

Divalent siRNAs are bioavailable in the lung and efficiently block SARS-CoV-2 infection

Supplementary Methods

Methods for designing SARS-CoV-2-targeting siRNAs Considering both Macro and Microevolution of the Virus

Phylogenetic Tree Construction

Closely related coronavirus species were selected based on prior analysis of the coronavirus lineage [57] to perform analysis of family homology. Genomic sequences of related coronaviruses and a representative group of five SARS-CoV-2 patient isolates (including the Wuhan-Hu-1 genome, which was our target sequence for siRNA design) were aligned using MAFFT [58]. We applied the rapid phylodynamic alignment pipeline included in the Augur package [59]. The phylogenetic tree was built using maximum likelihood with the Augur package following the RAxML (Randomized Axelerated Maximum Likelihood) method [60].

siRNA Selection

We designed SARS-CoV-2-targeting siRNAs with a twenty-nucleotide sequence containing a 16mer complementary region between positions 4 and 19 that is complementary to the target transcript. These siRNA sequences were then scored by their predicted efficiency to knockdown the target transcript. This scoring algorithm is described in greater detail elsewhere [36]. siRNAs containing the following features which predict poor functionality were excluded: a GC content greater than 56%, cross-reactivity (perfect complementarity through the 16mer complementary region) to any human transcripts, sequences containing microRNA seeds between positions 2 and 7 on the siRNA, and those containing stretches of five or more A's, U's, C's, or G's.

Since viral targets are known to mutate frequently, it is imperative to select siRNAs targeting regions that are predicted to remain constant. Regions least likely to mutate were identified as those with high homology to the genomes of 43 other closely related coronaviruses identified through localized genomic analysis [61] as this homology indicates low rates of mutation within these regions. We identify this as the "Family Homology" as this follows the macroevolution of the virus. The percent homology to the related coronavirus genomes were determined at every position for each of the SARS-CoV-2 target genes by comparing percentage homology to alignments of the six related coronavirus genomes at these positions. This was performed efficiently by conducting a multiple sequence alignment with the Clustal Omega Multiple Sequence Alignment tool [62] with default parameters. The percent homology to each related coronavirus were identified at each position of the SARS-CoV-2 genomic sequence using an alignment visualization tool such as the Jalview Viewer [63] with the SARS-CoV-2 sequence set as the consensus sequence. siRNA sequences were then ranked by their homology to the related coronavirus strains. This is straightforward as the siRNA sequences are derived directly from the SARS-CoV-2 genomic sequence (the consensus sequence for the alignment). The related

coronavirus genomes are fairly divergent from SARS-CoV-2 (~48% overall homology), and as such, few SARS-CoV-2-targeting siRNAs will have complete complementarity through the 16mer complementary region to all six related coronaviruses. Therefore, to identify siRNAs likely to target homologous regions, siRNAs were ranked first by the number of nucleotides within the sequence having a percentage homology greater than 70% within positions 3-9 and then by those with greater than 50% homology for at least 10 bases within the remaining positions of the 16mer complementary region. The top-ranking siRNAs were selected for further analysis.

To further optimize siRNA targeting of SARS-CoV-2, sequence data from SARS-CoV-2 isolates from COVID-19 patients were utilized to identify siRNAs that have the greatest potential to target a broad range of human-infecting SARS-CoV-2 variants. This we identify as the "Population Homology" as this follows the microevolution of the virus. These sequences were obtained from the GISAID Database [64], which at the time of analysis contained 53,792 such sequences. Note that not all SARS-CoV-2 sequences from patient isolates are high quality or complete genomes; sequences that are less than 97% complete (sequence length shorter than 29,000 nucleotides) and those containing >5% gaps of four nucleotides or more) were excluded from this analysis along with duplicate sequences. At the time of publication 45,668 sequences from patient isolates fit this criterion. To target only a portion of the SARS-CoV-2 genome rather than all nine transcripts, this criterion can be modified to include all isolates with sequences that are complete within the genomic region of interest. To identify siRNAs that target the greatest number of sequences from patient isolates, the sequences from the patient isolates were aligned with the target SARS-CoV-2 genomic sequence from which the siRNAs were derived using the Clustal Omega Multiple Sequence Alignment tool [62] with default parameters. The percent homology of each patient isolate sequence to the target SARS-CoV-2 genomic transcript were identified at each position of the SARS-CoV-2 genomic transcript. Targeting siRNAs were then scored by their percentage identity to the patient isolates. To do this we computed the normal of the 16mer complementary region by computing the sum of the squared percentage identities of the 16mer (Equation 1), with any 16mers overlaying with gaps being given a score of zero. The final score was computed by taking the square root of this value and dividing by the maximum homology value (400) to generate a homology percentage score. This scoring scheme was used to compute both the population homology score percent as well as the family homology score. The functionality score was normalized by the highest homology score to convert the value to percentages. The final score was a combination of the population and family homology scores with each contributing an equal component to the score as well as the functionality score (Equation 2). The top-ranking siRNAs were then selected. This is straightforward as the siRNA sequences are derived directly from the SARS-CoV-2 genomic sequence (the alignment consensus sequence). Commonly homology analyses utilize theoretical measures to perform homology scoring [65], however since siRNAs are designed to target the messenger RNA sequence directly, scoring based directly on the sequence is appropriate.

Equation 1. $Homology\ Score\ (\%) = 100\% \times \frac{\sqrt{\sum_{i=1}^{16}(Identity\ \%\ _i)^2}}{400}$

Equation 2. $Final\ Score\ (\%) = \frac{PH\ score\ (\%)}{4} + \frac{FH\ score\ (\%)}{4} + \frac{Funcitonality\ Score\ (\%)}{2}$

Normalized efficacy, population homology, and family homology scores were then compiled into a single final score. To compile, both homology scores were weighted by 0.5 while the efficacy score was weighted by 1 to ensure only functional siRNAs were selected [36]. This final score was used to select the top siRNA sequences, ten targeting each of the nine SARS-CoV-2 genes.

Oligonucleotide synthesis

Oligonucleotides were synthesized by phosphoramidite solid-phase synthesis on a Dr Oligo 48 (Biolytic, Fremont, CA), MerMade12 (Biosearch Technologies, Novato, CA) or AKTA Oligoplilot 10 (Cytiva, Marlborough, MA) using 2'-F-RNA, 2'-*O*-Me-RNA, LNA or DNA phosphoramidites with standard protecting groups. 5'-(*E*)-Vinyl tetra phosphonate (pivaloyloxymethyl) 2'-*O*-methyl-uridine 3'-CE phosphoramidite (VP) was purchased from Hongene Biotech, Union City, CA, Cy3 phosphoramidite (Quasar 570 CE) was purchased from GenePharma, Shanghai, China. Trivalent and tetravalent oligonucleotides were prepared using commercial trebler and doubler phosphoramidites, respectively, purchased from Glen Research, Sterling, VA. All other phosphoramidites used were purchased from ChemGenes, Wilmington, MA. Phosphoramidites were dissolved to 0.1 M in anhydrous acetonitrile (ACN), except for 2'-*O*-methyl-uridine phosphoramidite which was dissolved in anhydrous ACN containing 15% dimethylformamide. 5-(Benzylthio)-1*H*-tetrazole (BTT) was used as the activator at 0.25 M and the coupling time for all phosphoramidites was 4 min, except for trebler and doubler where the coupling time used was 8 min. Detritylations were performed using 3% trichloroacetic acid in dichloromethane. Capping reagents used were CAP A (20% n-methylimidazole in can) and CAP B (20% acetic anhydride and 30% 2,6-lutidine in ACN). Reagents for capping and detritylation were purchased from AIC, Westborough, MA. Phosphite oxidation to convert to phosphate was performed with 0.05 M iodine in pyridine-H_2O (9:1, v/v) or for phosphorothioate linkages the oxidation was performed with a 0.1 M solution of 3-[(dimethylaminomethylene)amino]-3*H*-1,2,4-dithiazole-5-thione (DDTT) in pyridine (ChemGenes) for 4 min. Unconjugated oligonucleotides were synthesized on 500Å (or 1000Å for trivalent and tetravalent oligonucleotides) long-chain alkyl amine (LCAA) controlled pore glass (CPG) functionalized with Unylinker terminus (ChemGenes). Cholesterol-conjugated oligonucleotides were synthesized on a 500Å LCAA-CPG support, where the cholesterol moiety is bound to tetra-ethylenglycol through a succinate linker (ChemGenes). Divalent oligonucleotides (DIO) were synthesized on modified solid support [43]. DCA and EPA conjugated oligonucleotides were synthesized on modified solid support [41].

Deprotection and purification of oligonucleotides for screening of sequences

Prior to the deprotection, synthesis columns containing oligonucleotides were treated with 10% diethylamine (DEA) in ACN to deprotect cyanoethyl groups. In synthesis columns, both unconjugated and cholesterol conjugated oligonucleotides on solid support were then deprotected with methylamine gas (Airgas, Radnor, PA) for an hour at room temperature. Deprotected oligonucleotides released from the solid support were precipitated on the support by passing

solution of (i) a mixture of 0.1 M sodium acetate in 85% ethanol and then (ii) 85% ethanol to the synthesis column. The excess ethanol on solid support was dried by air flow and the oligonucleotides were flushed out by passing water through the column. This procedure renders pure oligonucleotides used for *in vitro* experiments.

Deprotection and purification of oligonucleotides for *in vivo* experiments

Prior to the deprotection, oligonucleotides on solid support were treated with 10% DEA in ACN in synthesis columns to deprotect cyanoethyl groups. Cy3-labeled and non-labeled DCA and EPA conjugated oligonucleotides were cleaved and deprotected in 28-30% ammonium hydroxide-40% aq. methylamine (1:1, v/v) (AMA) for 2 hours at room temperature. Cy3-labeled and non-labeled unconjugated, divalent, trivalent and tetravalent oligonucleotides were cleaved and deprotected by AMA treatment for 2 hours at 45°C. The VP-containing oligonucleotides were not pretreated with DEA post-synthesis and were cleaved and deprotected as described previously [66]. Briefly, CPG with VP-oligonucleotides was treated with a solution of 3% DEA in 28-30% ammonium hydroxide at 35ºC for 20 hours.

All solutions containing cleaved oligonucleotides were filtered to remove the CPG and dried under vacuum. The resulting pellets were re-suspended in 5% ACN in water. Purifications were performed on an Agilent 1290 Infinity II HPLC system (Agilent, Santa Clara, CA). VP and non-labeled unconjugated, divalent, trivalent and tetravalent oligonucleotides were purified using a custom 20x150 mm column packed with Source 15Q anion exchange resin (Cytiva); running conditions: eluent A, 10 mM sodium acetate (pH 5) in 20% ACN in water; eluent B, 1 M sodium perchlorate in 20% ACN in water; linear gradient, 10 to 35% B in 40 min at 50°C. DCA, EPA conjugated and Cy3 labeled oligonucleotides were purified using a 21.2x150mm PRP-C18 column (Hamilton, Reno, NV); running conditions: eluent A, 50 mM sodium acetate (pH 6) in 5% ACN in water; eluent B, 100% ACN; linear gradient, 25 to 60% B in 40 min at 60°C. Flow was 30 mL/min in both methods and peaks were monitored at 260 nm for non-labeled oligonucleotides and 550 nm for labeled oligonucleotides. A separate column was used for Cy3-labeled oligonucleotides to avoid cross-contamination. Fractions were analyzed by liquid chromatography mass spectrometry (LC–MS), pure fractions combined and dried under vacuum. Oligonucleotides were re-suspended in 5% ACN and desalted by size exclusion on a 25×250 mm custom column packed with Sephadex G-25 media (Cytiva), and lyophilized.

LC–MS analysis of oligonucleotides

The identity of oligonucleotides was verified by LC–MS analysis on an Agilent 6530 accurate mass Q-TOF using the following conditions: buffer A: 100 mM 1,1,1,3,3,3-hexafluoroisopropanol (HFIP) and 9 mM triethylamine (TEA) in LC–MS grade water; buffer B:100 mM HFIP and 9 mM TEA in LC–MS grade methanol; column, Agilent AdvanceBio oligonucleotides C18; linear gradient 0–40% B 5 min (VP, unconjugated, DIO, trivalent and tetravalent); linear gradient 50-100% B 5 min (DCA, EPA conjugated and Cy3 labeled); temperature, 60°C; flow rate, 0.5 mL/min. LC peaks were monitored at 260 nm and for labeled oligonucleotides at 550 nm. MS parameters: Source, electrospray ionization; ion polarity, negative mode; range, 100–3, 200 m/z; scan rate, 2 spectra/s; capillary voltage, 4,000; fragmentor, 200 V; gas temp, 325°C.

Reagents for deprotection, purification and LC–MS were purchased from Fisher Scientific, Sigma Aldrich and Oakwood Chemicals.

A549$^{ACE2/TMPRSS2}$ clonal cell line generation and high ACE2-expressing cells generation

A549 cells (ATCC, cat#CCl-185) were cultured in 1X DMEM medium (Gibco, cat#11965-092) supplemented with 10% FBS (Gibco, cat#10437-028), 1x MEM NEAA (Gibco, cat#11140-050), 100 U/mL of penicillin-streptomycin (Corning, cat#30–002-CI), 1X sodium pyruvate (Gibco, cat#11360-070), and 1X Glutamax (Gibco, cat#35050-061) at 37°C and 5% CO_2. Cells were fed with fresh media every 2-3 days, and routinely checked for mycoplasma contamination. Lentivirus for ACE2 and TMPRSS2 was produced in HEK293T/17 (ATCC, cat#CRL-11268) with third generation lentiviral packaging plasmids pHDM-G, pHDM-Hgpm2, pHDM-tat1b, and pRC/CMV-rev1b (all from Dr. Maehr's lab) using TransIT-293 transfection reagent (Mirus, Madison, WI, cat#2700) according to the manufacturer′s recommendations. Following 48 hours of transfection, viral supernatant was collected, filtered, and stored at -80°C for later use. The A549$^{ACE2/TMPRSS2}$ clonal cell line was generated by transducing lentivirus expressing ACE2 and TMPRSS2 genes into the parental A549 cells. Transduced cells were selected with 1 μg/mL puromycin (Invitrogen, cat#A1113803) and screened for high SARS-CoV-2 infection clone as a result of the expression of ACE2 and TMPRSS2. To increase the virus infectivity, the cell populations with a higher ACE2 expression were further sorted using ACE2-specific antibody (AF933, R&D Systems). After puromycin selection, the infectivity significantly increased up to 40~60%.

Flow cytometry for lung siRNA distribution analysis

Collected mouse lung was dissociated to single-cell suspension using gentleMACS C Tubes (Miltenyi Biotec, Bergisch Gladbach, Germany) and a gentleMACS Octo Dissociator (Miltenyi Biotec) with the enzymatic dissociation solution containing 100 μL of Enzyme D, 15 μL of Enzyme A, 62.5 μL of Enzyme P (Miltenyi Biotec, Skeletal Muscle Dissociation Kit), 250 U/mL Collagenase IV (Worthington, Lakewood, NJ), and 2.3 mL of DMEM. Dissociated cells were filtered through a 70-μm strainer and red blood cells were lysed using ACK lysis buffer (155 mM NH_4Cl, 12 mM $NaHCO_3$, 0.1 mM EDTA in distilled water). Lung cells were stained at 4°C for 30 min with the following antibodies: VioGreen-conjugated CD45 antibody (Miltenyi Biotec, clone REA737), APC-conjugated CD31 antibody (Miltenyi Biotec, clone REA784), FITC-conjugated CD326 antibody (Miltenyi Biotec, clone REA977), PE-Vio770-conjugated CD140a antibody (Miltenyi Biotec, clone REA637), and PE-Vio615-conjugated MHCII antibody (Miltenyi Biotec, clone REA813). Cells were then washed twice and resuspended in the flow cytometry buffer containing 1 μM SYTOX Blue (Thermo Fisher Scientific). Stained cells were analyzed using a MACSQuant VYB flow cytometer (Miltenyi Biotec), and data were analyzed using FlowJo software (BD Biosciences, v10.6).

Serum cytokine analysis

The samples and standards were incubated, in duplicates, in a 96-well plate (Corning, Tewksbury, MA) with magnetic beads conjugated to antibodies against desired cytokines for two hours at room temperature with shaking at 500 rpm. Wells were then washed three times with wash buffer, using a magnetic plate washer (Bio-Rad). This step was followed by incubation with detection antibody

for one hour at room temperature with shaking. Following three washes, the samples were incubated with Streptavidin-PE for 30 min at room temperature with shaking. The samples were finally resuspended in 1X reading buffer after three washes. Plates were read in a MAGPIX® System instrument (Luminex Corporation). Standard curves were generated, and the levels of each cytokine were calculated using the 4-parameter logistic regression using GraphPad Prism 8.

Mouse-adapted SARS-CoV-2 infection and treatment studies

The *in vivo* infection studies were performed in an animal biosafety level 3 (ABSL3) facility in at UMass Chan Medical School. The study procedures were conducted with approval by the IACUC at UMass Chan Medical School. A total of 64 BALB/c mice (Jackson Laboratory, 8 week old females) were divided into 7 groups: group 1: PBS-treated, infected control (n=9); group 2: remdesivir-treated, infected (n=9); group 3: siRNA_NTC, infected (n=11); group 4: siRNA_orf7a_27751, infected (n=11); group 5: siRNA_N_29293, infected (n=11); group 6 1:1 mix of orf7a_27751 and N_29293, infected (n=11); group 7: uninfected, untreated control mice (n=3). Mice were anesthetized and inoculated intranasally with 1×10^4 plaque forming units of SARS-CoV-2 MA10. Mouse-adapted MA10 virus was obtained from BEI Resources (NR-55329). Remdesivir (VEKLURY) was purchased from the UMass Memorial Medical Center pharmacy and reconstituted in water for intraperitoneal administration. Mice were dosed twice daily (50 mg/kg/dose) x 4 days beginning at one day pre-infection. For siRNA, mice received intranasal injections (left nostril) of 20 nmol of siRNA at days -7, -4 and -1 before infection on day 0. Mice were weighed daily starting until end of study to measure infection-associated weight loss. At 3 days post-infection, mice were euthanized. The right lungs were collected and placed in 1 mL PBS with zirconium oxide beads and stored at –80°C for subsequent evaluation of lung virus titers. The left lungs were fixed in 10% neutral-formalin buffer at 4°C overnight for histopathology. For virus titer assays, lung homogenates were spun down at 10,000 x g for 5 min at 4°C. Supernatants were aliquoted in 500 µL and stored at -80°C until plaque assay. 200,000 Vero E6 cells per well were plated on a 12-well plate. The monolayer was washed once with PBS. Serial $\log_{10}$ diluted virus samples (320 µL) were placed in each well. The plate was incubated for 1 hour with rocking every 15 min to prevent drying of the cells. After adsorption, 2 mL carboxymethylcellulose overlay (1x MEM, 2% FBS, 2% carboxymethylcellulose) was placed in each well. The plate was incubated at 37°C for 3 days, after which 4% paraformaldehyde was added to each well and cells were stained with 1% crystal violet in 20% ethanol. For immunohistochemistry staining of SARS-CoV-2 nucleocapsid protein, sections were obtained from formalin-fixed, paraffin-embedded lung tissue and immunostained with SARS-CoV-2 nucleocapsid antibody (Sinobiological, cat#40143-MM05, at dilution 1:500 in 3% BSA) by the UMass Chan Medical School Morphology Core Facility.

Supplemental Table 1. Oligonucleotide duplexes used in *in vivo* studies. Information for each duplex is boxed with a thick outside border.
"P" denotes phosphate; "V" denotes vinyl phosphonate; "#" denotes phosphorothioate; "m" denotes 2*O*-methyl; "f" denotes 2'-fluoro; "l" denotes LNA; "A" denotes Adenosine; "U" denotes Uridine
G denotes Guanosine; "C" denotes Cytidine; "dA" denotes deoxyadenosine; "dT" denotes deoxythymidine; "dG" denotes deoxyguanosine; "dC" denotes deoxycytidine
"Teg" denotes triethylene glycol linker; "Chol" denotes cholesterol conjugate; "DCA" denotes C7 linker + docosanoic acid conjugate; "EPA" denotes C7 linker + eicosapentaenoic acid conjugate;
DIO denotes divalent spacer; "Tri" denotes trivalent spacer; "Tetra" denotes tetravalent spacer
"Cy3" denotes Cyanine3 fluorophore

siRNAs used in *in vitro* screens

siRNA Name	Target gene	Target sequence	siRNA guide strand sequence	siRNA passenger strand sequence
pp1a_416	pp1a	UGUGGCUUAGUAGAAGUUGA	P(mU)#(fC)#(mA)(mA)(mC)(fU)(mU)(mC)(mU)(mA)(mC)(mU)(mA)(fA)#(mG)#(fC)#(mC)#(mU)#(mU)#(mU)#(mU)	(mG)#(mC)#(mU)(mU)(mA)(fG)(fU)(fA)(mG)(fA)(mA)(mG)(mU)(mU)#(mG)#(mA)-TegChol
pp1a_2290	pp1a	UCAGACAUUCUUUAAGCUUG	P(mU)#(fA)#(mA)(mG)(mC)(fU)(mU)(mA)(mA)(mA)(mG)(mA)(mA)(fU)#(mG)#(fU)#(mC)#(mU)#(mU)#(mU)#(mU)	(mA)#(mC)#(mA)(mU)(mU)(fC)(fU)(fU)(mU)(fA)(mA)(mG)(mC)(mU)#(mU)#(mA)-TegChol
pp1a_6059	pp1a	UGUGAUAAUAUCAAAUUUGC	P(mU)#(fC)#(mA)(mA)(mA)(fU)(mU)(mU)(mG)(mA)(mU)(mA)(mU)(fU)#(mA)#(fU)#(mC)#(mU)#(mU)#(mU)#(mU)	(mA)#(mU)#(mA)(mA)(mU)(fA)(fU)(fC)(mA)(fA)(mA)(mU)(mU)(mU)#(mG)#(mA)-TegChol
pp1a_6322	pp1a	UGAAACAUCAAAUUCGUUUG	P(mU)#(fA)#(mA)(mA)(mC)(fG)(mA)(mA)(mU)(mU)(mU)(mG)(mA)(fU)#(mG)#(fU)#(mU)#(mU)#(mU)#(mU)#(mU)	(mA)#(mC)#(mA)(mU)(mC)(fA)(fA)(fA)(mU)(fU)(mC)(mG)(mU)(mU)#(mU)#(mA)-TegChol
pp1a_6499	pp1a	ACCAGCAAAUAAUAGUUUAA	P(mU)#(fU)#(mA)(mA)(mA)(fC)(mU)(mA)(mU)(mU)(mA)(mU)(mU)(fU)#(mG)#(fC)#(mU)#(mU)#(mU)#(mU)#(mU)	(mG)#(mC)#(mA)(mA)(mA)(fU)(fA)(fA)(mU)(fA)(mG)(mU)(mU)(mU)#(mA)#(mA)-TegChol
pp1a_7643	pp1a	GCUGGUAGUACAUUUAUUAG	P(mU)#(fU)#(mA)(mA)(mU)(fA)(mA)(mA)(mU)(mG)(mU)(mA)(mC)(fU)#(mA)#(fC)#(mC)#(mU)#(mU)#(mU)#(mU)	(mG)#(mU)#(mA)(mG)(mU)(fA)(fC)(fA)(mU)(fU)(mU)(mA)(mU)(mU)#(mA)#(mA)-TegChol
pp1a_8200	pp1a	UGUAGAAACUAAAGAUGUUG	P(mU)#(fA)#(mA)(mC)(mA)(fU)(mC)(mU)(mU)(mU)(mA)(mG)(mU)(fU)#(mU)#(fC)#(mU)#(mU)#(mU)#(mU)#(mU)	(mG)#(mA)#(mA)(mA)(mC)(fU)(fA)(fA)(mA)(fG)(mA)(mU)(mG)(mU)(mU)#(mA)#(mA)-TegChol
pp1a_8201	pp1a	GUAGAAACUAAAGAUGUUGU	P(mU)#(fC)#(mA)(mA)(mC)(fA)(mU)(mC)(mU)(mU)(mU)(mA)(mG)(fU)#(mU)#(fU)#(mC)#(mU)#(mU)#(mU)#(mU)	(mA)#(mA)#(mA)(mC)(mU)(fA)(fA)(fA)(mG)(fA)(mU)(mG)(mU)(mU)#(mG)#(mA)-TegChol
pp1a_8744	pp1a	UUUGCUAACAAACAUGCUGA	P(mU)#(fC)#(mA)(mG)(mC)(fA)(mU)(mG)(mU)(mU)(mU)(mG)(mU)(fU)#(mA)#(fG)#(mC)#(mU)#(mU)#(mU)#(mU)	(mC)#(mU)#(mA)(mA)(mC)(fA)(fA)(fA)(mC)(fA)(mU)(mG)(mC)(mU)#(mG)#(mA)-TegChol
pp1a_9679	pp1a	CUGGAUAACAAUUGCUUAUA	P(mU)#(fA)#(mU)(mA)(mA)(fG)(mC)(mA)(mA)(mU)(mU)(mG)(mU)(fU)#(mA)#(fU)#(mC)#(mU)#(mU)#(mU)#(mU)	(mA)#(mU)#(mA)(mA)(mC)(fA)(fA)(fU)(mU)(fG)(mC)(mU)(mU)(mA)#(mU)#(mA)-TegChol
pp1a_11594	pp1a	CAGUGUAUAAUGCUAGUUUA	P(mU)#(fA)#(mA)(mA)(mC)(fU)(mA)(mG)(mC)(mA)(mU)(mU)(mA)(fU)#(mA)#(fC)#(mA)#(mU)#(mU)#(mU)#(mU)	(mG)#(mU)#(mA)(mU)(mA)(fA)(fU)(fG)(mC)(fU)(mA)(mG)(mU)(mU)#(mU)#(mA)-TegChol
pp1a_12932	pp1a	CCUAAAGUGAAGUAUUUAUA	P(mU)#(fA)#(mU)(mA)(mA)(fA)(mU)(mA)(mC)(mU)(mU)(mC)(mA)(fC)#(mU)#(fU)#(mU)#(mU)#(mU)#(mU)#(mU)	(mA)#(mA)#(mG)(mU)(mG)(fA)(fA)(fG)(mU)(fA)(mU)(mU)(mU)(mA)#(mU)#(mA)-TegChol
pp1ab_14080	pp1ab	GGUAACUGGUAUGAUUUCGG	P(mU)#(fC)#(mG)(mA)(mA)(fA)(mU)(mC)(mA)(mU)(mA)(mC)(mC)(fA)#(mG)#(fU)#(mU)#(mU)#(mU)#(mU)#(mU)	(mA)#(mC)#(mU)(mG)(mG)(fU)(fA)(fU)(mG)(fA)(mU)(mU)(mU)(mC)#(mG)#(mA)-TegChol
pp1ab_14361	pp1ab	UCUGCAUUGUGCAAACUUUA	P(mU)#(fA)#(mA)(mA)(mG)(fU)(mU)(mU)(mG)(mC)(mA)(mC)(mA)(fA)#(mU)#(fG)#(mC)#(mU)#(mU)#(mU)#(mU)	(mC)#(mA)#(mU)(mU)(mG)(fU)(fG)(fC)(mA)(fA)(mA)(mC)(mU)(mU)#(mU)#(mA)-TegChol
pp1ab_14830	pp1ab	UGUGAUAUCAGACAACUACU	P(mU)#(fG)#(mU)(mA)(mG)(fU)(mU)(mG)(mU)(mC)(mU)(mG)(mA)(fU)#(mA)#(fU)#(mC)#(mU)#(mU)#(mU)#(mU)	(mA)#(mU)#(mA)(mU)(mC)(fA)(fG)(fA)(mC)(fA)(mA)(mC)(mU)#(mA)#(mC)#(mA)-TegChol
pp1ab_15376	pp1ab	UGUAGCUUGUCACACCGUUU	P(mU)#(fA)#(mA)(mC)(mG)(fG)(mU)(mG)(mU)(mG)(mA)(mC)(mA)(fA)#(mG)#(fC)#(mU)#(mU)#(mU)#(mU)	(mG)#(mC)#(mU)(mU)(mG)(fU)(fC)(fA)(mC)(fA)(mC)(mC)(mG)(mU)#(mU)#(mA)-TegChol
pp1ab_15786	pp1ab	UAAGUCAGUUCUUUAUUAUC	P(mU)#(fA)#(mU)(mA)(mA)(fU)(mA)(mA)(mA)(mG)(mA)(mA)(mC)(fU)#(mG)#(fA)#(mC)#(mU)#(mU)#(mU)#(mU)	(mU)#(mC)#(mA)(mG)(mU)(fU)(fC)(fU)(mU)(fU)(mA)(mU)(mU)(mA)#(mU)#(mA)-TegChol
pp1ab_17107	pp1ab	UUUGCUAUUGGCCUAGCUCU	P(mU)#(fG)#(mA)(mG)(mC)(fU)(mA)(mG)(mG)(mC)(mC)(mA)(mA)(fU)#(mA)#(fG)#(mC)#(mU)#(mU)#(mU)#(mU)	(mC)#(mU)#(mA)(mU)(mU)(fG)(fG)(fC)(mC)(fU)(mA)(mG)(mC)(mU)#(mC)#(mA)-TegChol
pp1ab_17370	pp1ab	GGCCACAAAUUAUGAUUUGA	P(mU)#(fC)#(mA)(mA)(mA)(fU)(mC)(mA)(mU)(mA)(mA)(mU)(mU)(fU)#(mG)#(fU)#(mG)#(mU)#(mU)#(mU)#(mU)	(mA)#(mC)#(mA)(mA)(mA)(fU)(fU)(fA)(mU)(fG)(mA)(mU)(mU)(mU)#(mG)#(mA)-TegChol
pp1ab_18025	pp1ab	GUGGCAACUUUACAAGCUGA	P(mU)#(fC)#(mA)(mG)(mC)(fU)(mU)(mG)(mU)(mA)(mA)(mG)(fU)#(mU)#(fG)#(mC)#(mU)#(mU)#(mU)#(mU)	(mC)#(mA)#(mA)(mC)(mU)(fU)(fU)(fA)(mC)(fA)(mA)(mG)(mC)(mU)#(mG)#(mA)-TegChol
pp1ab_18571	pp1ab	UCUGACAGAGUCGUAUUUGU	P(mU)#(fC)#(mA)(mA)(mA)(fU)(mA)(mC)(mG)(mA)(mC)(mU)(mC)(fU)#(mG)#(fU)#(mC)#(mU)#(mU)#(mU)#(mU)	(mA)#(mC)#(mA)(mG)(mA)(fG)(fU)(fC)(mG)(fU)(mA)(mU)(mU)(mU)#(mG)#(mA)-TegChol
pp1ab_20497	pp1ab	UCUGUUAUUGAUUUAUUACU	P(mU)#(fG)#(mU)(mA)(mA)(fU)(mA)(mA)(mA)(mU)(mC)(mA)(mA)(fU)#(mA)#(fA)#(mC)#(mU)#(mU)#(mU)#(mU)	(mU)#(mU)#(mA)(mU)(mU)(fG)(fA)(fU)(mU)(fU)(mA)(mU)(mU)(mA)#(mC)#(mA)-TegChol
pp1ab_20892	pp1ab	UGCACCAGGUACAGCUGUUU	P(mU)#(fA)#(mA)(mC)(mA)(fG)(mC)(mU)(mG)(mU)(mA)(mC)(mC)(fU)#(mG)#(fG)#(mU)#(mU)#(mU)#(mU)#(mU)	(mC)#(mC)#(mA)(mG)(mG)(fU)(fA)(fC)(mA)(fG)(mC)(mU)(mG)(mU)#(mU)#(mA)-TegChol
pp1ab_21391	pp1ab	UUUGACAUGAGUAAAUUUCC	P(mU)#(fG)#(mA)(mA)(mA)(fU)(mU)(mU)(mA)(mC)(mU)(mC)(mA)(fU)#(mG)#(fU)#(mC)#(mU)#(mU)#(mU)#(mU)	(mA)#(mC)#(mA)(mU)(mG)(fA)(fG)(fU)(mA)(fA)(mA)(mU)(mU)(mC)#(mG)#(mA)-TegChol
S_21944	spike	AUUAAAGUCUGUGAAUUUCA	P(mU)#(fG)#(mA)(mA)(mA)(fU)(mU)(mC)(mA)(mC)(mA)(mG)(mA)(fC)#(mU)#(fU)#(mU)#(mU)#(mU)#(mU)	(mA)#(mA)#(mG)(mU)(mC)(fU)(fG)(fU)(mG)(fA)(mA)(mU)(mU)(mU)#(mC)#(mA)-TegChol
S_22223	spike	UCGGCUUUAGAACCAUUGGU	P(mU)#(fC)#(mC)(mA)(mA)(fU)(mG)(mG)(mU)(mU)(mC)(mU)(mA)(fA)#(mA)#(fG)#(mC)#(mU)#(mU)#(mU)#(mU)	(mC)#(mU)#(mU)(mU)(mA)(fG)(fA)(fA)(mC)(fC)(mA)(mU)(mU)(mG)#(mG)#(mA)-TegChol
S_22550	spike	CCUAAUAUUACAAACUUGUG	P(mU)#(fA)#(mC)(mA)(mA)(fG)(mU)(mU)(mU)(mG)(mU)(mA)(mA)(fU)#(mA)#(fU)#(mU)#(mU)#(mU)#(mU)#(mU)	(mA)#(mU)#(mA)(mA)(mU)(mU)(fA)(fC)(fA)(mA)(fA)(mC)(mU)(mU)(mG)#(mU)#(mA)-TegChol
S_22820	spike	GAUUAUAAUUAUAAAUUACC	P(mU)#(fG)#(mU)(mA)(mA)(fU)(mU)(mU)(mA)(mU)(mA)(mA)(mU)(fU)#(mA)#(fU)#(mA)#(mU)#(mU)#(mU)#(mU)	(mA)#(mU)#(mA)(mA)(mU)(fU)(fA)(fU)(mA)(fA)(mA)(mU)(mU)(mA)#(mC)#(mA)-TegChol
S_22898	spike	GGUGGUAAUUAUAAUUACCU	P(mU)#(fG)#(mG)(mU)(mA)(fA)(mU)(mU)(mA)(mA)(mU)(mU)(fU)#(mA)#(fC)#(mC)#(mU)#(mU)#(mU)#(mU)	(mG)#(mU)#(mA)(mA)(mU)(fU)(fA)(fU)(mA)(fA)(mU)(mU)(mA)#(mC)#(mC)#(mA)-TegChol
S_23174	spike	UGUGUCAAUUUCAACUUCAA	P(mU)#(fU)#(mG)(mA)(mA)(fG)(mU)(mU)(mG)(mA)(mA)(mA)(mU)(fU)#(mG)#(fA)#(mC)#(mU)#(mU)#(mU)#(mU)	(mU)#(mC)#(mA)(mA)(mU)(fU)(fU)(fC)(mA)(fA)(mC)(mU)(mU)(mC)#(mA)#(mA)-TegChol
S_23239	spike	UCUGCCUUUCCAACAAUUUG	P(mU)#(fA)#(mA)(mA)(mU)(fU)(mG)(mU)(mU)(mG)(mG)(mA)(mA)(fA)#(mG)#(fG)#(mC)#(mU)#(mU)#(mU)#(mU)	(mC)#(mC)#(mU)(mU)(mU)(fC)(fC)(fA)(mA)(fC)(mA)(mA)(mU)(mU)#(mU)#(mA)-TegChol
S_23240	spike	CUGCCUUUCCAACAAUUUGG	P(mU)#(fC)#(mA)(mA)(mA)(fU)(mU)(mG)(mU)(mU)(mG)(mG)(mA)(fA)#(mA)#(fG)#(mG)#(mU)#(mU)#(mU)#(mU)	(mC)#(mU)#(mU)(mU)(mU)(mC)(fC)(fA)(fA)(mC)(fA)(mA)(mU)(mU)(mU)#(mG)#(mA)-TegChol
S_23774	spike	UGUACAAUGUACAUUUGUGG	P(mU)#(fC)#(mA)(mC)(mA)(fA)(mA)(mU)(mG)(mU)(mU)(mA)(mC)(mA)(fU)#(mU)#(fG)#(mU)#(mU)#(mU)#(mU)	(mC)#(mA)#(mA)(mU)(mG)(fU)(fA)(fC)(mA)(fU)(mU)(mU)(mG)(mU)#(mG)#(mA)-TegChol
S_24056	spike	GGCUUCAUCAAACAAUAUGG	P(mU)#(fC)#(mA)(mU)(mA)(fU)(mU)(mG)(mU)(mU)(mU)(mG)(mA)(fU)#(mG)#(fA)#(mA)#(mU)#(mU)#(mU)#(mU)	(mU)#(mC)#(mA)(mU)(mC)(fA)(fA)(fA)(mC)(fA)(mA)(mU)(mA)(mU)#(mG)#(mA)-TegChol
S_24289	spike	UGGAGUUACACAGAAUGUUC	P(mU)#(fA)#(mA)(mC)(mA)(fU)(mU)(mC)(mU)(mG)(mU)(mG)(mU)(fA)#(mA)#(fC)#(mU)#(mU)#(mU)#(mU)#(mU)	(mG)#(mU)#(mU)(mA)(mC)(fA)(fC)(fA)(mG)(fA)(mA)(mU)(mG)(mU)#(mU)#(mA)-TegChol
S_25375	spike	UUACACAUAAACGAACUUAU	P(mU)#(fU)#(mA)(mA)(mG)(fU)(mU)(mC)(mG)(mU)(mU)(mU)(mA)(fU)#(mG)#(fU)#(mG)#(mU)#(mU)#(mU)#(mU)	(mA)#(mC)#(mA)(mU)(mA)(fA)(fA)(fC)(mG)(fA)(mA)(mC)(mU)(mU)#(mA)#(mA)-TegChol
3a_25413	orf3a	CUUCACAAUUGGAACUGUAA	P(mU)#(fU)#(mA)(mC)(mA)(fG)(mU)(mU)(mC)(mC)(mA)(mA)(mU)(fU)#(mG)#(fU)#(mG)#(mU)#(mU)#(mU)#(mU)	(mA)#(mC)#(mA)(mA)(mU)(fU)(fG)(fG)(mA)(fA)(mC)(mU)(mG)(mU)#(mA)#(mA)-TegChol
3a_25630	orf3a	GUUUGCAACUUGCUGUUGUU	P(mU)#(fA)#(mC)(mA)(mA)(fC)(mA)(mG)(mC)(mA)(mA)(mG)(mU)(fU)#(mG)#(fC)#(mA)#(mU)#(mU)#(mU)#(mU)	(mG)#(mC)#(mA)(mA)(mC)(fU)(fU)(fG)(mC)(fU)(mG)(mU)(mU)(mG)#(mU)#(mA)-TegChol
3a_25717	orf3a	UAUGCUUUAGUCUACUUCUU	P(mU)#(fA)#(mG)(mA)(mA)(fG)(mU)(mA)(mG)(mA)(mC)(mU)(mA)(fA)#(mA)#(fG)#(mC)#(mU)#(mU)#(mU)#(mU)	(mC)#(mU)#(mU)(mU)(mA)(fG)(fU)(fC)(mU)(fA)(mC)(mU)(mU)(mC)#(mU)#(mA)-TegChol
3a_25734	orf3a	CUUGCAGAGUAUAAACUUUG	P(mU)#(fA)#(mA)(mA)(mG)(fU)(mU)(mU)(mA)(mU)(mA)(mC)(mU)(fC)#(mU)#(fG)#(mC)#(mU)#(mU)#(mU)#(mU)	(mC)#(mA)#(mG)(mA)(mG)(fU)(fA)(fU)(mA)(fA)(mA)(mC)(mU)(mU)#(mU)#(mA)-TegChol
3a_25736	orf3a	UGCAGAGUAUAAACUUUGUA	P(mU)#(fA)#(mC)(mA)(mA)(fA)(mG)(mU)(mU)(mU)(mA)(mU)(mA)(fC)#(mU)#(fC)#(mU)#(mU)#(mU)#(mU)#(mU)	(mG)#(mA)#(mG)(mU)(mA)(fU)(fA)(fA)(mA)(fC)(mU)(mU)(mU)(mG)#(mU)#(mA)-TegChol
3a_25745	orf3a	UAAACUUUGUAAGAAUAAUA	P(mU)#(fA)#(mU)(mU)(mA)(fU)(mU)(mC)(mU)(mU)(mA)(mC)(mA)(fA)#(mA)#(fG)#(mU)#(mU)#(mU)#(mU)	(mC)#(mU)#(mU)(mU)(mG)(fU)(fA)(fA)(mG)(fA)(mA)(mU)(mA)(mA)#(mU)#(mA)-TegChol
3a_25868	orf3a	CUUACAAUAGUGUAACUUCU	P(mU)#(fG)#(mA)(mA)(mG)(fU)(mU)(mA)(mC)(mA)(mC)(mU)(fU)#(mG)#(fU)#(mU)#(mU)#(mU)#(mU)#(mU)	(mC)#(mA)#(mA)(mU)(mA)(fG)(fU)(fG)(mU)(fA)(mA)(mC)(mU)(mU)#(mC)#(mA)-TegChol
3a_25870	orf3a	UACAAUAGUGUAACUUCUUC	P(mU)#(fA)#(mA)(mG)(mA)(fA)(mG)(mU)(mU)(mA)(mC)(mA)(mC)(fU)#(mA)#(fU)#(mU)#(mU)#(mU)#(mU)	(mA)#(mU)#(mA)(mG)(mU)(fG)(fU)(fA)(mA)(fC)(mU)(mU)(mC)(mU)#(mU)#(mA)-TegChol
3a_25914	orf3a	CACAACAAGUCCUAUUUCUG	P(mU)#(fA)#(mG)(mA)(mA)(fA)(mU)(mA)(mG)(mG)(mA)(mC)(mU)(fU)#(mG)#(fU)#(mU)#(mU)#(mU)#(mU)	(mA)#(mC)#(mA)(mA)(mG)(fU)(fC)(fC)(mU)(fA)(mU)(mU)(mU)(mC)#(mU)#(mA)-TegChol
3a_25992	orf3a	UGUUGUAUUACACAGUUACU	P(mU)#(fG)#(mU)(mA)(mA)(fC)(mU)(mG)(mU)(mG)(mU)(mA)(mA)(fU)#(mA)#(fC)#(mA)#(mU)#(mU)#(mU)#(mU)	(mG)#(mU)#(mA)(mU)(mU)(fA)(fC)(fA)(mC)(fA)(mG)(mU)(mU)(mA)#(mC)#(mA)-TegChol
3a_26018	orf3a	CAGACUAUUACCAGCUGUAC	P(mU)#(fU)#(mA)(mC)(mA)(fG)(mC)(mU)(mG)(mG)(mU)(mA)(mA)(fU)#(mA)#(fG)#(mU)#(mU)#(mU)#(mU)	(mC)#(mU)#(mA)(mU)(mA)(fU)(fG)(mC)(mU)(mG)(mG)(mU)(mA)#(mA)#(mA)-TegChol
3a_26066	orf3a	UUGAACAUGUUACCUUCUUC	P(mU)#(fA)#(mA)(mG)(mA)(fA)(mG)(mG)(mU)(mA)(mA)(mC)(mA)(fU)#(mG)#(fU)#(mU)#(mU)#(mU)#(mU)	(mA)#(mC)#(mA)(mU)(mG)(fU)(fU)(fA)(mC)(fC)(mU)(mU)(mC)(mU)#(mU)#(mA)-TegChol
E_26258	envelope	UUUCGGAAGAGACAGGUACG	P(mU)#(fG)#(mU)(mA)(mC)(fC)(mU)(mG)(mU)(mC)(mU)(mC)(mU)(fU)#(mC)#(fC)#(mG)#(mU)#(mU)#(mU)#(mU)	(mG)#(mG)#(mA)(mA)(mG)(fA)(fG)(fA)(mC)(fA)(mG)(mG)(mU)(mA)#(mC)#(mA)-TegChol
E_26261	envelope	CGGAAGAGACAGGUACGUUA	P(mU)#(fA)#(mA)(mC)(mG)(fU)(mA)(mC)(mC)(mU)(mG)(mU)(mC)(fU)#(mC)#(fU)#(mU)#(mU)#(mU)#(mU)	(mA)#(mG)#(mA)(mG)(mA)(fC)(fA)(fG)(mG)(fU)(mA)(mC)(mG)(mU)#(mU)#(mA)-TegChol
E_26269	envelope	ACAGGUACGUUAAUAGUUAA	P(mU)#(fU)#(mA)(mA)(mC)(fU)(mA)(mU)(mU)(mA)(mA)(mC)(mG)(fU)#(mA)#(fC)#(mC)#(mU)#(mU)#(mU)#(mU)	(mG)#(mU)#(mA)(mC)(mG)(fU)(fU)(fA)(mA)(fU)(mA)(mG)(mU)(mU)#(mA)#(mA)-TegChol
E_26277	envelope	GUUAAUAGUUAAUAGCGUAC	P(mU)#(fU)#(mA)(mC)(mG)(fC)(mU)(mA)(mU)(mU)(mA)(mA)(mC)(fU)#(mA)#(fU)#(mU)#(mU)#(mU)#(mU)	(mA)#(mU)#(mA)(mG)(mU)(fU)(fA)(fA)(mU)(fA)(mG)(mC)(mG)(mU)#(mA)#(mA)-TegChol

E_26305	envelope	CUUGCUUUCGUGGUAUUCUU	P(mU)#(fA)#(mG)(mA)(mA)(fU)(mA)(mC)(mC)(mA)(mC)(mG)(mA)(fA)#(mA)#(fG)#(mC)#(mU)#(mU)#(mU)#(mU)	(mC)#(mU)#(mU)(mU)(mC)(fG)(fU)(fG)(mG)(fU)(mA)(mU)(mU)(mC)#(mU)#(mA)-TegChol
E_26313	envelope	CGUGGUAUUCUUGCUAGUUA	P(mU)#(fA)#(mA)(mC)(mU)(fA)(mG)(mC)(mA)(mA)(mG)(mA)(mU)(fU)#(mA)#(fC)#(mC)#(mU)#(mU)#(mU)#(mU)	(mG)#(mU)#(mA)(mU)(mU)(mC)(fC)(fU)(fU)(mG)(fC)(mU)(mA)(mG)(mU)#(mU)#(mA)-TegChol
E_26369	envelope	ACUGCUGCAAUAUUGUUAAC	P(mU)#(fU)#(mU)(mA)(mA)(fC)(mA)(mA)(mU)(mA)(mU)(mU)(mG)(fC)#(mA)#(fG)#(mC)#(mU)#(mU)#(mU)#(mU)	(mC)#(mU)#(mG)(mC)(mA)(fA)(fU)(fA)(mA)(fU)(mG)(mU)(mU)(mA)#(mA)#(mA)-TegChol
E_26374	envelope	UGCAAUAUUGUUAACGUGAG	P(mU)#(fU)#(mC)(mA)(mC)(fG)(mU)(mU)(mA)(mA)(mC)(mA)(mA)(fU)#(mA)#(fU)#(mU)#(mU)#(mU)#(mU)#(mU)	(mA)#(mU)#(mA)(mU)(mU)(fG)(fU)(fU)(mA)(fA)(mC)(mG)(mU)(mG)#(mA)#(mA)-TegChol
E_26455	envelope	CCUGAUCUUCUGGUCUAAAC	P(mU)#(fU)#(mU)(mU)(mA)(fG)(mA)(mC)(mC)(mA)(mG)(mA)(mA)(fG)#(mA)#(fU)#(mC)#(mU)#(mU)#(mU)#(mU)	(mA)#(mU)#(mC)(mU)(mU)(fC)(fU)(fG)(mG)(fU)(mC)(mU)(mA)(mA)#(mA)#(mA)-TegChol
E_26463	envelope	UCUGGUCUAAACGAACUAAA	P(mU)#(fU)#(mU)(mA)(mG)(fU)(mU)(mC)(mG)(mU)(mU)(mU)(mA)(fG)#(mA)#(fC)#(mC)#(mU)#(mU)#(mU)#(mU)	(mG)#(mU)#(mC)(mU)(mA)(fA)(fA)(fC)(mG)(fA)(mA)(mC)(mU)(mA)#(mA)#(mA)-TegChol
E_26467	envelope	GUCUAAACGAACUAAAUAUU	P(mU)#(fA)#(mU)(mA)(mU)(fU)(mU)(mA)(mG)(mU)(mU)(mC)(mG)(fU)#(mA)#(fU)#(mA)#(mU)#(mU)#(mU)#(mU)	(mA)#(mA)#(mA)(mC)(mG)(fA)(fA)(fC)(mU)(fA)(mA)(mA)(mU)(mA)#(mU)#(mA)-TegChol
E_26470	envelope	UAAACGAACUAAAUAUUAUA	P(mU)#(fA)#(mU)(mA)(mA)(fU)(mA)(mU)(mU)(mU)(mA)(mG)(mU)(fU)#(mC)#(fG)#(mU)#(mU)#(mU)#(mU)#(mU)	(mC)#(mG)#(mA)(mA)(mC)(fU)(fA)(fA)(mA)(fU)(mA)(mU)(mU)(mA)#(mU)#(mA)-TegChol
M_26573	membrane	UGAACAAUGGAACCUAGUAA	P(mU)#(fU)#(mA)(mC)(mU)(fA)(mG)(mG)(mU)(mU)(mC)(mC)(mA)(fU)#(mU)#(fG)#(mU)#(mU)#(mU)#(mU)#(mU)	(mC)#(mA)#(mA)(mU)(mG)(fG)(fA)(fA)(mC)(fC)(mU)(mA)(mG)(mU)#(mA)#(mA)-TegChol
M_26581	membrane	GGAACCUAGUAAUAGGUUUC	P(mU)#(fA)#(mA)(mA)(mC)(fC)(mU)(mA)(mU)(mU)(mA)(mC)(mU)(fA)#(mG)#(fG)#(mU)#(mU)#(mU)#(mU)#(mU)	(mC)#(mC)#(mU)(mA)(mG)(fU)(fA)(fA)(mU)(fA)(mG)(mG)(mU)(mU)#(mU)#(mA)-TegChol
M_26602	membrane	UAUUCCUUACAUGGAUUUGU	P(mU)#(fC)#(mA)(mA)(mA)(fU)(mC)(mC)(mA)(mU)(mG)(mU)(mA)(fA)#(mG)#(fG)#(mA)#(mU)#(mU)#(mU)#(mU)	(mC)#(mC)#(mU)(mU)(mA)(fC)(fA)(fU)(mG)(fG)(mA)(mU)(mU)#(mG)#(mA)-TegChol
M_26624	membrane	UCUACAAUUUGCCUAUGCCA	P(mU)#(fG)#(mG)(mC)(mA)(fU)(mA)(mG)(mG)(mC)(mA)(mA)(mA)(fU)#(mU)#(fG)#(mU)#(mU)#(mU)#(mU)#(mU)	(mC)#(mA)#(mA)(mU)(mU)(fU)(fG)(fC)(mC)(fU)(mA)(mU)(mG)(mC)#(mC)#(mA)-TegChol
M_26637	membrane	UAUGCCAACAGGAAUAGGUU	P(mU)#(fA)#(mC)(mC)(mU)(fA)(mU)(mU)(mC)(mC)(mU)(mG)(mU)(fU)#(mG)#(fG)#(mC)#(mU)#(mU)#(mU)#(mU)	(mC)#(mC)#(mA)(mA)(mC)(fA)(fG)(fG)(mA)(fA)(mU)(mA)(mG)(mG)#(mU)#(mA)-TegChol
M_26638	membrane	AUGCCAACAGGAAUAGGUUU	P(mU)#(fA)#(mA)(mC)(mC)(fU)(mA)(mU)(mU)(mC)(mC)(mU)(mG)(fU)#(mU)#(fG)#(mG)#(mU)#(mU)#(mU)#(mU)	(mC)#(mA)#(mA)(mC)(mA)(fG)(fG)(fA)(mA)(fU)(mA)(mG)(mG)(mU)#(mU)#(mA)-TegChol
M_26693	membrane	AUGGCCAGUAACUUUAGCUU	P(mU)#(fA)#(mG)(mC)(mU)(fA)(mA)(mA)(mG)(mU)(mU)(mA)(mC)(fU)#(mG)#(fG)#(mC)#(mU)#(mU)#(mU)#(mU)	(mC)#(mC)#(mA)(mG)(mU)(fA)(fA)(fC)(mU)(fU)(mU)(mA)(mG)(mC)#(mU)#(mA)-TegChol
M_26717	membrane	UGUGCUUGCUGCUGUUUACA	P(mU)#(fG)#(mU)(mA)(mA)(fA)(mC)(mA)(mG)(mC)(mA)(mG)(mC)(fA)#(mA)#(fG)#(mC)#(mU)#(mU)#(mU)#(mU)	(mC)#(mU)#(mU)(mG)(mC)(fU)(fG)(fC)(mU)(fG)(mU)(mU)(mA)#(mC)#(mA)-TegChol
M_27014	membrane	GCCUAAAGAAAUCACUGUUG	P(mU)#(fA)#(mA)(mC)(mA)(fG)(mU)(mG)(mA)(mU)(mU)(mU)(mC)(fU)#(mU)#(fU)#(mA)#(mU)#(mU)#(mU)#(mU)	(mA)#(mA)#(mA)(mG)(mA)(fA)(fA)(fU)(mC)(fA)(mC)(mU)(mG)(mU)#(mU)#(mA)-TegChol
M_27032	membrane	UGCUACAUCACGAACGCUUU	P(mU)#(fA)#(mA)(mG)(mC)(fG)(mU)(mU)(mC)(mG)(mU)(mG)(mA)(fU)#(mG)#(fU)#(mA)#(mU)#(mU)#(mU)#(mU)	(mA)#(mC)#(mA)(mU)(mC)(fA)(fC)(fG)(mA)(fA)(mC)(mG)(mC)(mU)#(mU)#(mA)-TegChol
M_27035	membrane	UACAUCACGAACGCUUUCUU	P(mU)#(fA)#(mG)(mA)(mA)(fA)(mG)(mC)(mG)(mU)(mU)(mC)(mG)(fU)#(mG)#(fA)#(mU)#(mU)#(mU)#(mU)#(mU)	(mU)#(mC)#(mA)(mC)(mG)(fA)(fA)(fC)(mG)(fC)(mU)(mU)(mU)(mC)#(mU)#(mA)-TegChol
M_27123	orf7a	AUUGGCAACUAUAAAUUAAA	P(mU)#(fU)#(mU)(mA)(mA)(fU)(mU)(mU)(mA)(mU)(mG)(mU)(fU)#(mG)#(fC)#(mC)#(mU)#(mU)#(mU)#(mU)	(mG)#(mC)#(mA)(mA)(mC)(fU)(fA)(fU)(mA)(fA)(mA)(mA)(mU)(mA)#(mC)#(mA)-TegChol
7a_27455	orf7a	AAGAGUGUGUUAGAGGUACA	P(mU)#(fG)#(mU)(mA)(mC)(fC)(mU)(mC)(mU)(mA)(mA)(mC)(mA)(fC)#(mA)#(fC)#(mU)#(mU)#(mU)#(mU)	(mG)#(mU)#(mG)(mU)(mG)(fU)(fU)(fA)(mG)(fA)(mG)(mG)(mU)(mA)#(mC)#(mA)-TegChol
7a_27522	orf7a	UUCACCAUUUCAUCCUCUAG	P(mU)#(fU)#(mA)(mG)(mA)(fG)(mG)(mA)(mU)(mG)(mA)(mA)(mA)(fU)#(mG)#(fG)#(mU)#(mU)#(mU)#(mU)#(mU)	(mC)#(mC)#(mA)(mU)(mU)(fU)(fC)(fA)(mU)(fC)(mC)(mU)(mC)(mU)#(mA)#(mA)-TegChol
7a_27537	orf7a	UCUAGCUGAUAACAAAUUUG	P(mU)#(fA)#(mA)(mA)(mU)(fU)(mU)(mG)(mU)(mU)(mA)(mU)(mC)(fA)#(mG)#(fC)#(mU)#(mU)#(mU)#(mU)	(mG)#(mC)#(mU)(mG)(mA)(fU)(fA)(fA)(mC)(fA)(mA)(mA)(mU)(mU)#(mU)#(mA)-TegChol
7a_27553	orf7a	UUUGCACUGACUUGCUUUAG	P(mU)#(fU)#(mA)(mA)(mA)(fG)(mC)(mA)(mA)(mG)(mU)(mC)(mA)(fG)#(mU)#(fG)#(mC)#(mU)#(mU)#(mU)#(mU)	(mC)#(mA)#(mC)(mU)(mG)(fA)(fC)(fU)(mU)(fG)(mC)(mU)(mU)(mU)#(mA)#(mA)-TegChol
7a_27565	orf7a	UGCUUUAGCACUCAAUUUGC	P(mU)#(fC)#(mA)(mA)(mA)(fU)(mU)(mG)(mA)(mG)(mU)(mG)(mC)(fU)#(mA)#(fA)#(mA)#(mU)#(mU)#(mU)#(mU)	(mU)#(mU)#(mA)(mG)(mC)(fA)(fC)(fU)(mC)(fA)(mA)(mU)(mU)(mG)#(mA)-TegChol
7a_27633	orf7a	AUCAGUUUCACCUAAACUGU	P(mU)#(fC)#(mA)(mG)(mU)(fU)(mU)(mA)(mG)(mG)(mU)(mG)(mA)(fA)#(mA)#(fC)#(mU)#(mU)#(mU)#(mU)	(mG)#(mU)#(mU)(mU)(mC)(fA)(fC)(fC)(mU)(fA)(mA)(mA)(mC)(mU)#(mG)#(mA)-TegChol
7a_27656	orf7a	UCAGACAAGAGGAAGUUCAA	P(mU)#(fU)#(mG)(mA)(mA)(fC)(mU)(mU)(mC)(mC)(mU)(mC)(mU)(fU)#(mG)#(fU)#(mC)#(mU)#(mU)#(mU)#(mU)	(mA)#(mC)#(mA)(mA)(mG)(fA)(fG)(fG)(mA)(fA)(mG)(mU)(mU)(mC)#(mA)#(mA)-TegChol
7a_27671	orf7a	UUCAAGAACUUUACUCUCCA	P(mU)#(fG)#(mG)(mA)(mG)(fA)(mG)(mU)(mA)(mA)(mA)(mG)(mU)(fU)#(mC)#(fU)#(mU)#(mU)#(mU)#(mU)#(mU)	(mA)#(mG)#(mA)(mA)(mC)(fU)(fU)(fU)(mA)(fC)(mU)(mC)(mU)(mC)#(mC)#(mA)-TegChol
7a_27705	orf7a	UGCGGCAAUAGUGUUUAUAA	P(mU)#(fU)#(mA)(mU)(mA)(fA)(mA)(mC)(mA)(mC)(mU)(mA)(mU)(fU)#(mG)#(fC)#(mC)#(mU)#(mU)#(mU)#(mU)	(mG)#(mC)#(mA)(mA)(mU)(fA)(fG)(fU)(mG)(fU)(mU)(mU)(mA)(mU)#(mA)#(mA)-TegChol
7a_27715	orf7a	GUGUUUAUAACACUUUGCUU	P(mU)#(fA)#(mG)(mC)(mA)(fA)(mA)(mG)(mU)(mG)(mU)(mU)(mA)(fU)#(mA)#(fA)#(mA)#(mU)#(mU)#(mU)#(mU)	(mU)#(mU)#(mA)(mU)(mA)(fA)(fC)(fA)(mC)(fU)(mU)(mU)(mG)(mC)#(mU)#(mA)-TegChol
7a_27720	orf7a	UAUAACACUUUGCUUCACAC	P(mU)#(fU)#(mG)(mU)(mG)(fA)(mA)(mG)(mC)(mA)(mA)(mA)(mG)(fU)#(mG)#(fU)#(mU)#(mU)#(mU)#(mU)#(mU)	(mA)#(mC)#(mA)(mC)(mU)(fU)(fU)(fG)(mC)(fU)(mU)(mC)(mA)(mC)#(mA)#(mA)-TegChol
7a_27751	orf7a	ACAGAAUGAUUGAACUUUCA	P(mU)#(fG)#(mA)(mA)(mA)(fG)(mU)(mU)(mC)(mA)(mA)(mU)(mC)(fA)#(mU)#(fU)#(mC)#(mU)#(mU)#(mU)#(mU)	(mA)#(mA)#(mU)(mG)(mA)(fU)(fU)(fG)(mA)(fA)(mC)(mU)(mU)(mU)#(mC)#(mA)-TegChol
8b_27932	orf8b	AGCUGCAUUUCACCAAGAAU	P(mU)#(fU)#(mU)(mC)(mU)(fU)(mG)(mG)(mU)(mG)(mA)(mA)(mA)(fU)#(mG)#(fC)#(mA)#(mU)#(mU)#(mU)#(mU)	(mG)#(mC)#(mA)(mU)(mU)(fU)(fC)(fA)(mC)(fC)(mA)(mA)(mG)(mA)#(mA)#(mA)-TegChol
8b_27940	orf8b	UUCACCAAGAAUGUAGUUUA	P(mU)#(fA)#(mA)(mA)(mC)(fU)(mA)(mC)(mA)(mU)(mU)(mC)(mU)(fU)#(mG)#(fG)#(mU)#(mU)#(mU)#(mU)	(mC)#(mC)#(mA)(mA)(mA)(mG)(fA)(fA)(fU)(mG)(fU)(mA)(mG)(mU)(mU)#(mU)#(mA)-TegChol
8b_27986	orf8b	UGUAGUUGAUGACCCGUGUC	P(mU)#(fA)#(mC)(mA)(mC)(fG)(mG)(mG)(mU)(mC)(mA)(mU)(mC)(fA)#(mA)#(fC)#(mU)#(mU)#(mU)#(mU)	(mG)#(mU)#(mU)(mG)(mA)(fU)(fG)(fA)(mC)(fC)(mC)(mG)(mU)(mG)#(mU)#(mA)-TegChol
8b_28002	orf8b	UGUCCUAUUCACUUCUAUUC	P(mU)#(fA)#(mA)(mU)(mA)(fG)(mA)(mA)(mG)(mU)(mG)(mA)(mA)(fU)#(mA)#(fG)#(mG)#(mU)#(mU)#(mU)#(mU)	(mC)#(mU)#(mA)(mU)(mU)(fC)(fA)(fC)(mU)(fU)(mC)(mU)(mA)(mU)#(mU)#(mA)-TegChol
8b_28024	orf8b	AAUGGUAUAUUAGAGUAGGA	P(mU)#(fC)#(mC)(mU)(mA)(fC)(mU)(mC)(mU)(mA)(mA)(mU)(mA)(fU)#(mA)#(fC)#(mC)#(mU)#(mU)#(mU)#(mU)	(mG)#(mU)#(mA)(mU)(mA)(fU)(fU)(fA)(mG)(fA)(mG)(mU)(mA)(mG)#(mG)#(mA)-TegChol
8b_28091	orf8b	UUCUAAAUCACCCAUUCAGU	P(mU)#(fC)#(mU)(mG)(mA)(fA)(mU)(mG)(mG)(mU)(mG)(mA)(fU)#(mA)#(fU)#(mU)#(mU)#(mU)#(mU)#(mU)	(mA)#(mA)#(mA)(mU)(mC)(fA)(fC)(fC)(mC)(fA)(mU)(mU)(mC)(mA)#(mG)#(mA)-TegChol
8b_28119	orf8b	AUCGGUAAUUAUACAGUUUC	P(mU)#(fA)#(mA)(mA)(mC)(fU)(mG)(mU)(mA)(mU)(mA)(mA)(mU)(fU)#(mA)#(fC)#(mC)#(mU)#(mU)#(mU)#(mU)	(mG)#(mU)#(mA)(mA)(mA)(mU)(fU)(fA)(fU)(mA)(fC)(mA)(mG)(mU)(mU)#(mU)#(mA)-TegChol
8b_28127	orf8b	UUAUACAGUUUCCUGUUUAC	P(mU)#(fU)#(mA)(mA)(mA)(fC)(mA)(mG)(mG)(mA)(mA)(mA)(mC)(fU)#(mG)#(fU)#(mA)#(mU)#(mU)#(mU)#(mU)	(mA)#(mC)#(mA)(mG)(mU)(fU)(fU)(fC)(mC)(fU)(mG)(mU)(mU)(mU)#(mA)#(mA)-TegChol
8b_28128	orf8b	UAUACAGUUUCCUGUUUACC	P(mU)#(fG)#(mU)(mA)(mA)(fA)(mC)(mA)(mG)(mG)(mA)(mA)(mA)(fC)#(mU)#(fG)#(mU)#(mU)#(mU)#(mU)#(mU)	(mC)#(mA)#(mG)(mU)(mU)(fU)(fC)(fC)(mU)(fG)(mU)(mU)(mU)(mA)#(mC)#(mA)-TegChol
8b_28163	orf8b	CCAGGAACCUAAAUUGGGUA	P(mU)#(fA)#(mC)(mC)(mC)(fA)(mA)(mU)(mU)(mU)(mA)(mG)(mG)(fU)#(mU)#(fC)#(mC)#(mU)#(mU)#(mU)#(mU)	(mG)#(mA)#(mA)(mC)(mC)(fU)(fA)(fA)(mA)(fU)(mU)(mG)(mG)(mG)#(mU)#(mA)-TegChol
8b_28218	orf8b	UUAGAGUAUCAUGACGUUCG	P(mU)#(fG)#(mA)(mA)(mC)(fG)(mU)(mC)(mA)(mU)(mG)(mA)(fU)#(mC)#(fU)#(mC)#(mU)#(mU)#(mU)#(mU)	(mA)#(mG)#(mU)(mA)(mU)(fC)(fA)(fU)(mG)(fG)(mA)(mC)(mG)(mU)(mU)#(mC)#(mA)-TegChol
8b_28222	orf8b	AGUAUCAUGACGUUCGUGUU	P(mU)#(fA)#(mC)(mA)(mC)(fG)(mA)(mA)(mC)(mG)(mU)(mC)(mA)(fU)#(mG)#(fA)#(mU)#(mU)#(mU)#(mU)	(mU)#(mC)#(mA)(mU)(mG)(fA)(fC)(fG)(mU)(fU)(mC)(mG)(mU)(mG)#(mU)#(mA)-TegChol
N_28407	nucleocapsid	UACCCAAUAAUACUGCGUCU	P(mU)#(fG)#(mA)(mC)(mG)(fC)(mA)(mG)(mU)(mA)(mU)(mU)(mA)(fU)#(mU)#(fG)#(mG)#(mU)#(mU)#(mU)#(mU)	(mC)#(mA)#(mA)(mU)(mA)(fA)(fU)(fA)(mC)(fU)(mG)(mC)(mG)(mU)#(mC)#(mA)-TegChol
N_28655	nucleocapsid	GACGGCAUCAUAUGGGUUGC	P(mU)#(fC)#(mA)(mA)(mC)(fC)(mC)(mA)(mU)(mA)(mU)(mG)(mA)(fU)#(mG)#(fC)#(mC)#(mU)#(mU)#(mU)#(mU)	(mG)#(mC)#(mA)(mU)(mC)(fA)(fU)(fA)(mU)(fG)(mG)(mG)(mU)(mU)#(mG)#(mA)-TegChol
N_28945	nucleocapsid	UGACAGAUUGAACCAGCUUG	P(mU)#(fA)#(mA)(mG)(mC)(fU)(mG)(mG)(mU)(mU)(mC)(mA)(mA)(fU)#(mC)#(fU)#(mG)#(mU)#(mU)#(mU)#(mU)	(mA)#(mG)#(mA)(mU)(mU)(fG)(fA)(fA)(mC)(fC)(mC)(mU)(mU)#(mA)#(mG)-TegChol
N_28992	nucleocapsid	AACAACAAGGCCAAACUGUC	P(mU)#(fA)#(mC)(mA)(mG)(fU)(mU)(mU)(mG)(mG)(mC)(mC)(mU)(fU)#(mG)#(fU)#(mU)#(mU)#(mU)#(mU)	(mA)#(mC)#(mA)(mA)(mG)(fG)(fC)(fC)(mA)(fA)(mA)(mC)(mU)(mG)#(mU)#(mA)-TegChol
N_29141	nucleocapsid	GAACUAAUCAGACAAGGAAC	P(mU)#(fU)#(mU)(mC)(mC)(fU)(mU)(mG)(mU)(mC)(mU)(mG)(mA)(fU)#(mU)#(fA)#(mG)#(mU)#(mU)#(mU)#(mU)	(mU)#(mA)#(mA)(mU)(mC)(fA)(fG)(fA)(mC)(fA)(mA)(mG)(mG)(mA)#(mA)#(mA)-TegChol
N_29276	nucleocapsid	GGUGCCAUCAAAUUGGAUGA	P(mU)#(fC)#(mA)(mU)(mC)(fC)(mA)(mA)(mU)(mU)(mU)(mG)(mA)(fU)#(mG)#(fG)#(mC)#(mU)#(mU)#(mU)#(mU)	(mC)#(mC)#(mA)(mU)(mC)(fA)(fA)(fA)(mU)(fU)(mG)(mG)(mA)(mU)#(mG)#(mA)-TegChol
N_29292	nucleocapsid	AUGACAAAGAUCCAAAUUUC	P(mU)#(fA)#(mA)(mA)(mU)(fU)(mU)(mG)(mG)(mA)(mU)(mC)(mU)(fU)#(mU)#(fG)#(mU)#(mU)#(mU)#(mU)#(mU)	(mC)#(mA)#(mA)(mA)(mG)(fA)(fU)(fC)(mC)(fA)(mA)(mA)(mU)(mU)#(mU)#(mA)-TegChol
N_29293	nucleocapsid	UGACAAAGAUCCAAAUUUCA	P(mU)#(fG)#(mA)(mA)(mA)(fU)(mU)(mU)(mG)(mG)(mA)(mU)(mC)(fU)#(mU)#(fU)#(mG)#(mU)#(mU)#(mU)#(mU)	(mA)#(mA)#(mA)(mG)(mA)(fU)(fC)(fC)(mA)(fA)(mA)(mU)(mU)#(mC)#(mA)-TegChol
N_29303	nucleocapsid	CCAAAUUUCAAAGAUCAAGU	P(mU)#(fC)#(mU)(mU)(mG)(fA)(mU)(mC)(mU)(mU)(mU)(mG)(mA)(fA)#(mA)#(fU)#(mU)#(mU)#(mU)#(mU)	(mA)#(mU)#(mU)(mU)(mC)(fA)(fA)(fA)(mG)(fA)(mU)(mC)(mA)(mA)#(mG)#(mA)-TegChol
N_29307	nucleocapsid	AUUUCAAAGAUCAAGUCAUU	P(mU)#(fA)#(mU)(mG)(mA)(fC)(mU)(mU)(mG)(mA)(mU)(mC)(mU)(fU)#(mU)#(fG)#(mA)#(mU)#(mU)#(mU)#(mU)	(mC)#(mA)#(mA)(mA)(mG)(fA)(fU)(fC)(mA)(fA)(mG)(mU)(mC)(mA)#(mU)#(mA)-TegChol
N_29328	nucleocapsid	UGCUGAAUAAGCAUAUUGAC	P(mU)#(fU)#(mC)(mA)(mA)(fU)(mA)(mU)(mG)(mC)(mU)(mA)(fU)#(mU)#(fC)#(mA)#(mU)#(mU)#(mU)#(mU)	(mG)#(mA)#(mA)(mU)(mA)(fA)(fG)(fC)(mA)(fU)(mA)(mU)(mU)(mG)#(mA)#(mA)-TegChol
N_29464	nucleocapsid	UGCAGAUUUGGAUGAUUUCU	P(mU)#(fG)#(mA)(mA)(fU)(fU)(mC)(mA)(mU)(mC)(mC)(mA)(fA)#(mU)#(fC)#(mU)#(mU)#(mU)#(mU)#(mU)	(mG)#(mA)#(mU)(mU)(mU)(fG)(fG)(fA)(mU)(fG)(mA)(mU)(mU)(mC)#(mA)-TegChol
HTT_10150	Huntingtin	UAUAUCAGUAAAGAGAUUAA	P(mU)#(fU)#(mA)(mA)(mU)(fC)(mU)(mC)(mU)(mU)(mU)(mA)(mC)(fU)#(mG)#(fA)#(mU)#(mU)#(mU)#(mU)#(mU)	(mU)#(mC)#(mA)(mG)(mU)(fA)(fA)(fA)(mG)(fA)(mG)(mA)(mU)(mU)#(mA)#(mA)-TegChol
NTC	n/a	n/a	P(mU)#(fA)#(mA)(mU)(mC)(fG)(mU)(mA)(mU)(mU)(mU)(mG)(mU)(fC)#(mA)#(fA)#(mU)#(mC)#(mA)#(fU)#(mA)	(mG)#(mA)#(mU)(mU)(mU)(fG)(fG)(fA)(mU)(fG)(mA)(mU)(mU)(mU)#(mC)#(mA)-TegChol

ASOs used in *in vitro* screens

ASO Name	Target gene	Target sequence	ASO sequence

pp1a_417	pp1a	ACUUCUACUAAGCCAC	(1A)#(1C)#(1T)#(dT)#(d5C)#(dT)#(dA)#(d5C)#(dT)#(dA)#(dA)#(dG)#(d5C)#(1C)#(1A)#(1C)
pp1a_2293	pp1a	AAGCUUAAAGAAUGUC	(1A)#(1A)#(1G)#(d5C)#(dT)#(dT)#(dA)#(dA)#(dA)#(dG)#(dA)#(dA)#(dT)#(1G)#(1T)#(1C)
pp1a_8745	pp1a	GCAUGUUUGUUAGCAA	(1G)#(1C)#(1A)#(dT)#(dG)#(dT)#(dT)#(dT)#(dG)#(dT)#(dT)#(dA)#(dG)#(1C)#(1A)#(1A)
pp1a_8747	pp1a	CAGCAUGUUUGUUAGC	(1C)#(1A)#(1G)#(d5C)#(dA)#(dT)#(dG)#(dT)#(dT)#(dT)#(dG)#(dT)#(dT)#(1A)#(1G)#(1C)
pp1a_9680	pp1a	AAGCAAUUGUUAUCCA	(1A)#(1A)#(1G)#(d5C)#(dA)#(dA)#(dT)#(dT)#(dG)#(dT)#(dT)#(dA)#(dT)#(1C)#(1C)#(1A)
pp1a_9681	pp1a	UAAGCAAUUGUUAUCC	(1T)#(1A)#(1A)#(dG)#(d5C)#(dA)#(dA)#(dT)#(dT)#(dG)#(dT)#(dT)#(dA)#(1T)#(1C)#(1C)
pp1ab_14361	pp1ab	GUUUGCACAAUGCAGA	(1G)#(1T)#(1T)#(dT)#(dG)#(d5C)#(dA)#(d5C)#(dA)#(dA)#(dT)#(dG)#(d5C)#(1A)#(1G)#(1A)
pp1ab_17111	pp1ab	AGAGCUAGGCCAAUAG	(1A)#(1G)#(1A)#(dG)#(d5C)#(dT)#(dA)#(dG)#(dG)#(d5C)#(d5C)#(dA)#(dA)#(1T)#(1A)#(1G)
pp1ab_18027	pp1ab	AGCUUGUAAAGUUGCC	(1A)#(1G)#(1C)#(dT)#(dT)#(dG)#(dT)#(dA)#(dA)#(dA)#(dG)#(dT)#(dT)#(1G)#(1C)#(1C)
pp1ab_20893	pp1ab	CAGCUGUACCUGGUGC	(1C)#(1A)#(1G)#(d5C)#(dT)#(dG)#(dT)#(dA)#(d5C)#(d5C)#(dT)#(dG)#(dG)#(1T)#(1G)#(1C)
pp1ab_20894	pp1ab	ACAGCUGUACCUGGUG	(1A)#(1C)#(1A)#(dG)#(d5C)#(dT)#(dG)#(dT)#(dA)#(d5C)#(d5C)#(dT)#(dG)#(1G)#(1T)#(1G)
pp1ab_20895	pp1ab	AACAGCUGUACCUGGU	(1A)#(1A)#(1C)#(dA)#(dG)#(d5C)#(dT)#(dG)#(dT)#(dA)#(d5C)#(d5C)#(dT)#(1G)#(1G)#(1T)
S_22224	spike	AAUGGUUCUAAAGCCG	(1A)#(1A)#(1T)#(dG)#(dG)#(dT)#(dT)#(d5C)#(dT)#(dA)#(dA)#(dA)#(dG)#(1C)#(1C)#(1G)
S_22225	spike	CAAUGGUUCUAAAGCC	(1C)#(1A)#(1A)#(dT)#(dG)#(dG)#(dT)#(dT)#(d5C)#(dT)#(dA)#(dA)#(dA)#(1G)#(1C)#(1C)
S_23177	spike	UGAAGUUGAAAUUGAC	(1T)#(1G)#(1A)#(dA)#(dG)#(dT)#(dT)#(dG)#(dA)#(dA)#(dA)#(dT)#(dT)#(1G)#(1A)#(1C)
S_23778	spike	CCACAAAUGUACAUUG	(1C)#(1C)#(1A)#(d5C)#(dA)#(dA)#(dA)#(dT)#(dG)#(dT)#(dA)#(d5C)#(dA)#(1T)#(1T)#(1G)
S_25376	spike	AGUUCGUUUAUGUGUA	(1A)#(1G)#(1T)#(dT)#(d5C)#(dG)#(dT)#(dT)#(dT)#(dA)#(dT)#(dG)#(dT)#(1G)#(1T)#(1A)
S_25378	spike	UAAGUUCGUUUAUGUG	(1T)#(1A)#(1A)#(dG)#(dT)#(dT)#(d5C)#(dG)#(dT)#(dT)#(dT)#(dA)#(dT)#(1G)#(1T)#(1G)
3a_25719	orf3a	GAAGUAGACUAAAGCA	(1G)#(1A)#(1A)#(dG)#(dT)#(dA)#(dG)#(dA)#(d5C)#(dT)#(dA)#(dA)#(dA)#(1G)#(1C)#(1A)
3a_25914	orf3a	AAUAGGACUUGUUGUG	(1A)#(1A)#(1T)#(dA)#(dG)#(dG)#(dA)#(d5C)#(dT)#(dT)#(dG)#(dT)#(dT)#(1G)#(1T)#(1G)
3a_25993	orf3a	AACUGUGUAAUACAAC	(1A)#(1A)#(1C)#(dT)#(dG)#(dT)#(dG)#(dT)#(dA)#(dA)#(dT)#(dA)#(d5C)#(1A)#(1A)#(1C)
3a_26019	orf3a	CAGCUGGUAAUAGUCU	(1C)#(1A)#(1G)#(d5C)#(dT)#(dG)#(dG)#(dT)#(dA)#(dA)#(dT)#(dA)#(dG)#(1T)#(1C)#(1T)
3a_26020	orf3a	ACAGCUGGUAAUAGUC	(1A)#(1C)#(1A)#(dG)#(d5C)#(dT)#(dG)#(dG)#(dT)#(dA)#(dA)#(dT)#(dA)#(1G)#(1T)#(1C)
3a_26021	orf3a	UACAGCUGGUAAUAGU	(1T)#(1A)#(1C)#(dA)#(dG)#(d5C)#(dT)#(dG)#(dG)#(dT)#(dA)#(dA)#(dT)#(1A)#(1G)#(1T)
E_26260	envelope	UACCUGUCUCUUCCGA	(1T)#(1A)#(1C)#(d5C)#(dT)#(dG)#(dT)#(d5C)#(dT)#(d5C)#(dT)#(dT)#(d5C)#(1C)#(1G)#(1A)
E_26265	envelope	UAACGUACCUGUCUCU	(1T)#(1A)#(1A)#(d5C)#(dG)#(dT)#(dA)#(d5C)#(d5C)#(dT)#(dG)#(dT)#(d5C)#(1T)#(1C)#(1T)
E_26370	envelope	AACAAUAUUGCAGCAG	(1A)#(1A)#(1C)#(dA)#(dA)#(dT)#(dA)#(dT)#(dT)#(dG)#(d5C)#(dA)#(dG)#(1C)#(1A)#(1G)
E_26371	envelope	UAACAAUAUUGCAGCA	(1T)#(1A)#(1A)#(d5C)#(dA)#(dA)#(dT)#(dA)#(dT)#(dT)#(dG)#(d5C)#(dA)#(1G)#(1C)#(1A)
E_26374	envelope	CGUUAACAAUAUUGCA	(1C)#(1G)#(1T)#(dT)#(dA)#(dA)#(d5C)#(dA)#(dA)#(dT)#(dA)#(dT)#(dT)#(1G)#(1C)#(1A)
E_26378	envelope	CUCACGUUAACAAUAU	(1C)#(1T)#(1C)#(dA)#(d5C)#(dG)#(dT)#(dT)#(dA)#(dA)#(d5C)#(dA)#(dA)#(1T)#(1A)#(1T)
M_26582	membrane	ACCUAUUACUAGGUUC	(1A)#(1C)#(1C)#(dT)#(dA)#(dT)#(dT)#(dA)#(d5C)#(dT)#(dA)#(dG)#(dG)#(1T)#(1T)#(1C)
M_26584	membrane	AAACCUAUUACUAGGU	(1A)#(1A)#(1A)#(d5C)#(d5C)#(dT)#(dA)#(dT)#(dT)#(dA)#(d5C)#(dT)#(dA)#(1G)#(1G)#(1T)
M_26605	membrane	CAAAUCCAUGUAAGGA	(1C)#(1A)#(1A)#(dA)#(dT)#(d5C)#(d5C)#(dA)#(dT)#(dG)#(dT)#(dA)#(dA)#(1G)#(1G)#(1A)
M_26606	membrane	ACAAAUCCAUGUAAGG	(1A)#(1C)#(1A)#(dA)#(dA)#(dT)#(d5C)#(d5C)#(dA)#(dT)#(dG)#(dT)#(dA)#(1A)#(1G)#(1G)
M_26628	membrane	UGGCAUAGGCAAAUUG	(1T)#(1G)#(1G)#(d5C)#(dA)#(dT)#(dA)#(dG)#(dG)#(d5C)#(dA)#(dA)#(dA)#(1T)#(1T)#(1G)
M_26720	membrane	GUAAACAGCAGCAAGC	(1G)#(1T)#(1A)#(dA)#(dA)#(d5C)#(dA)#(dG)#(d5C)#(dA)#(dG)#(d5C)#(dA)#(1A)#(1G)#(1C)
7a_27458	orf7a	GUACCUCUAACACACU	(1G)#(1T)#(1A)#(d5C)#(d5C)#(dT)#(d5C)#(dT)#(dA)#(dA)#(d5C)#(dA)#(d5C)#(1A)#(1C)#(1T)
7a_27553	orf7a	AGCAAGUCAGUGCAAA	(1A)#(1G)#(1C)#(dA)#(dA)#(dG)#(dT)#(d5C)#(dA)#(dG)#(dT)#(dG)#(d5C)#(1A)#(1A)#(1A)
7a_27565	orf7a	AUUGAGUGCUAAAGCA	(1A)#(1T)#(1T)#(dG)#(dA)#(dG)#(dT)#(dG)#(d5C)#(dT)#(dA)#(dA)#(dA)#(1G)#(1C)#(1A)
7a_27569	orf7a	GCAAAUUGAGUGCUAA	(1G)#(1C)#(1A)#(dA)#(dA)#(dT)#(dT)#(dG)#(dA)#(dG)#(dT)#(dG)#(d5C)#(1T)#(1A)#(1A)
7a_27705	orf7a	AAACACUAUUGCCGCA	(1A)#(1A)#(1A)#(d5C)#(dA)#(d5C)#(dT)#(dA)#(dT)#(dT)#(dG)#(d5C)#(d5C)#(1G)#(1C)#(1A)
7a_27724	orf7a	GUGUGAAGCAAAGUGU	(1G)#(1T)#(1G)#(dT)#(dG)#(dA)#(dA)#(dG)#(d5C)#(dA)#(dA)#(dA)#(dG)#(1T)#(1G)#(1T)
8b_28002	orf8b	AGAAGUGAAUAGGACA	(1A)#(1G)#(1A)#(dA)#(dG)#(dT)#(dG)#(dA)#(dA)#(dT)#(dA)#(dG)#(dG)#(1A)#(1C)#(1A)
8b_28092	orf8b	GAAUGGGUGAUUUAGA	(1G)#(1A)#(1A)#(dT)#(dG)#(dG)#(dG)#(dT)#(dG)#(dA)#(dT)#(dT)#(dT)#(1A)#(1G)#(1A)
8b_28093	orf8b	UGAAUGGGUGAUUUAG	(1T)#(1G)#(1A)#(dA)#(dT)#(dG)#(dG)#(dG)#(dT)#(dG)#(dA)#(dT)#(dT)#(1T)#(1A)#(1G)
8b_28122	orf8b	AAACUGUAUAAUUACC	(1A)#(1A)#(1A)#(d5C)#(dT)#(dG)#(dT)#(dA)#(dT)#(dA)#(dA)#(dT)#(dT)#(1A)#(1C)#(1C)
8b_28165	orf8b	CCCAAUUUAGGUUCCU	(1C)#(1C)#(1C)#(dA)#(dA)#(dT)#(dT)#(dT)#(dA)#(dG)#(dG)#(dT)#(dT)#(1C)#(1C)#(1T)
N_28656	nucleocapsid	ACCCAUAUGAUGCCGU	(1A)#(1C)#(1C)#(d5C)#(dA)#(dT)#(dA)#(dT)#(dG)#(dA)#(dT)#(dG)#(d5C)#(1C)#(1G)#(1T)
N_28946	nucleocapsid	GCUGGUUCAAUCUGUC	(1G)#(1C)#(1T)#(dG)#(dG)#(dT)#(dT)#(d5C)#(dA)#(dA)#(dT)#(d5C)#(dT)#(1G)#(1T)#(1C)
N_28949	nucleocapsid	CAAGCUGGUUCAAUCU	(1C)#(1A)#(1A)#(dG)#(d5C)#(dT)#(dG)#(dG)#(dT)#(dT)#(d5C)#(dA)#(dA)#(1T)#(1C)#(1T)
N_29141	nucleocapsid	CUUGUCUGAUUAGUUC	(1C)#(1T)#(1T)#(dG)#(dT)#(d5C)#(dT)#(dG)#(dA)#(dT)#(dT)#(dA)#(dG)#(1T)#(1T)#(1C)
N_29142	nucleocapsid	CCUUGUCUGAUUAGUU	(1C)#(1C)#(1T)#(dT)#(dG)#(dT)#(d5C)#(dT)#(dG)#(dA)#(dT)#(dT)#(dA)#(1G)#(1T)#(1T)
N_29311	nucleocapsid	AAUGACUUGAUCUUUG	(1A)#(1A)#(1T)#(dG)#(dA)#(d5C)#(dT)#(dT)#(dG)#(dA)#(dT)#(d5C)#(dT)#(1T)#(1T)#(1G)
NTC	n/a	n/a	(1A)#(1T)#(1T)#(dT)#(dT)#(dA)#(dT)#(dT)#(dC)#(dG)#(dG)#(dA)#(1G)#(1C)#(1T)

siRNA used for mouse tissue distribution and efficacy studies

siRNA Name	Target gene	Target sequence	siRNA guide strand sequence	siRNA passenger strand sequence
HTT10150 - Monovalent	huntingtin	UAUAUCAGUAAAGAGAUUAA	V(mU)#(fU)#(mA)(fA)(mU)(fC)(mU)(fC)(mU)(fU)(mU)(fA)(mC)#(fU)#(mG)#(fA)#(mU)#(fA)#(mU)#(fA)	Cy3-(fC)#(mA)#(fG)(mU)(fA)(mA)(fA)(mG)(fA)(mG)(fA)(mU)(fU)#(mA)#(fA)
HTT10150 - Divalent	huntingtin	UAUAUCAGUAAAGAGAUUAA	V(mU)#(fU)#(mA)(fA)(mU)(fC)(mU)(fC)(mU)(fU)(mU)(fA)(mC)#(fU)#(mG)#(fA)#(mU)#(fA)#(mU)#(fA)	Cy3-(fC)#(mA)#(fG)(mU)(fA)(mA)(fA)(mG)(fA)(mG)(fA)(mU)(fU)#(mA)#(fA)-DIO
HTT10150 - Trivalent	huntingtin	UAUAUCAGUAAAGAGAUUAA	V(mU)#(fU)#(mA)(fA)(mU)(fC)(mU)(fC)(mU)(fU)(mU)(fA)(mC)#(fU)#(mG)#(fA)#(mU)#(fA)#(mU)#(fA)	Cy3-(fC)#(mA)#(fG)(mU)(fA)(mA)(fA)(mG)(fA)(mG)(fA)(mU)(fU)#(mA)#(fA)-Tri
HTT10150 - Tetravalent	huntingtin	UAUAUCAGUAAAGAGAUUAA	V(mU)#(fU)#(mA)(fA)(mU)(fC)(mU)(fC)(mU)(fU)(mU)(fA)(mC)#(fU)#(mG)#(fA)#(mU)#(fA)#(mU)#(fA)	Cy3-(fC)#(mA)#(fG)(mU)(fA)(mA)(fA)(mG)(fA)(mG)(fA)(mU)(fU)#(mA)#(fA)(dT)(dT)-Tetra

HTT10150 - DCA	huntingtin	UAUAUCAGUAAAGAGAUUAA	V(mU)#(fU)#(mA)(fA)(mU)(fC)(mU)(fC)(mU)(fU)(mU)(fA)(mC)#(fU)#(mG)#(fA)#(mU)#(fA)#(mU)#(fA)	Cy3-(fC)#(mA)#(fG)(mU)(fA)(mA)(fA)(mG)(fA)(mG)(fA)(mU)(fU)#(mA)#(fA)(dT)(dT)-DCA
HTT10150 - EPA	huntingtin	UAUAUCAGUAAAGAGAUUAA	V(mU)#(fU)#(mA)(fA)(mU)(fC)(mU)(fC)(mU)(fU)(mU)(fA)(mC)#(fU)#(mG)#(fA)#(mU)#(fA)#(mU)#(fA)	Cy3-(fC)#(mA)#(fG)(mU)(fA)(mA)(fA)(mG)(fA)(mG)(fA)(mU)(fU)#(mA)#(fA)(dT)(dT)-EPA
CD47 - Monovalent	cd47	CAUGUCACAUAAAUGAUUAC	V(mU)#(fU)#(mA)(fA)(fU)(fC)(mA)(fU)(mU)(fU)(mA)(fU)(mG)(fU)#(mG)#(fA)#(mC)#(mU)#(mU)#(mU)#(mU)	(mU)#(mC)#(mA)(fC)(mA)(fU)(mA)(fA)(mA)(fU)(mG)(mA)(mU)(fU)#(mA)#(mA)
CD47 - Divalent	cd47	CAUGUCACAUAAAUGAUUAC	V(mU)#(fU)#(mA)(fA)(fU)(fC)(mA)(fU)(mU)(fU)(mA)(fU)(mG)(fU)#(mG)#(fA)#(mC)#(mU)#(mU)#(mU)#(mU)	(mU)#(mC)#(mA)(fC)(mA)(fU)(mA)(fA)(mA)(fU)(mG)(mA)(mU)(fU)#(mA)#(mA)-DIO
CD47 - Trivalent	cd47	CAUGUCACAUAAAUGAUUAC	V(mU)#(fU)#(mA)(fA)(fU)(fC)(mA)(fU)(mU)(fU)(mA)(fU)(mG)(fU)#(mG)#(fA)#(mC)#(mU)#(mU)#(mU)#(mU)	(mU)#(mC)#(mA)(fC)(mA)(fU)(mA)(fA)(mA)(fU)(mG)(mA)(mU)(fU)#(mA)#(mA)-Tri
CD47 - Tetravalent	cd47	CAUGUCACAUAAAUGAUUAC	V(mU)#(fU)#(mA)(fA)(fU)(fC)(mA)(fU)(mU)(fU)(mA)(fU)(mG)(fU)#(mG)#(fA)#(mC)#(mU)#(mU)#(mU)#(mU)	(mU)#(mC)#(mA)(fC)(mA)(fU)(mA)(fA)(mA)(fU)(mG)(mA)(mU)(fU)#(mA)#(mA)-Tetra
NTC - Divalent	n/a	n/a	V(mU)#(fA)#(mA)(fU)(fC)(fG)(mU)(fA)(mU)(fU)(mU)(fG)(mU)#(fC)#(mA)#(fA)#(mU)#(mC)#(mA)#(fU)	(mU)#(mG)#(fA)(mC)(fA)(mA)(fA)(mU)(fA)(mC)(mG)(mA)(fU)#(mU)#(mA)-DIO

siRNA used for mouse tissue distribution and efficacy studies

siRNA Name	Target gene	Target sequence	siRNA guide strand sequence	siRNA passenger strand sequence
pp1a_2290 - Divalent	pp1a	UCAGACAUUCUUUAAGCUUG	V(mU)#(fA)#(mA)(fG)(fC)(fU)(mU)(fA)(mA)(fA)(mG)(fA)(mA)(fU)#(mG)#(fU)#(mC)#(mU)#(mU)#(mU)#(mU)	(mA)#(mC)#(mA)(fU)(mU)(fC)(mU)(fU)(mU)(fA)(mA)(mG)(mC)(fU)#(mU)#(mA)-DIO
pp1ab_18571 - Divalent	pp1ab	UCUGACAGAGUCGUAUUUGU	V(mU)#(fC)#(mA)(fA)(fA)(fU)(mA)(fC)(mG)(fA)(mC)(fU)(mC)(fU)#(mG)#(fU)#(mC)#(mU)#(mU)#(mU)#(mU)	(mA)#(mC)#(mA)(fG)(mA)(fG)(mU)(fC)(mG)(fU)(mA)(mU)(mU)(fU)#(mG)#(mA)-DIO
orf7a_27751 - Divalent	orf7a	ACAGAAUGAUUGAACUUUCA	V(mU)#(fG)#(mA)(fA)(fA)(fG)(mU)(fU)(mC)(fA)(mA)(fU)(mC)(fA)#(mU)#(fU)#(mC)#(mU)#(mU)#(mU)#(mU)	(mA)#(mA)#(mU)(fG)(mA)(fU)(mU)(fG)(mA)(fA)(mC)(mU)(mU)(fU)#(mC)#(mA)-DIO
N_29293 - Divalent	nucleocapsid	UGACAAAGAUCCAAAUUUCA	V(mU)#(fG)#(mA)(fA)(fA)(fU)(mU)(fU)(mG)(fG)(mA)(fU)(mC)(fU)#(mU)#(fU)#(mG)#(mU)#(mU)#(mU)#(mU)	(mA)#(mA)#(mA)(fG)(mA)(fU)(mC)(fC)(mA)(fA)(mA)(mU)(mU)(fU)#(mC)#(mA)-DIO
NTC - Divalent	n/a	n/a	V(mU)#(fA)#(mA)(fU)(fC)(fG)(mU)(fA)(mU)(fU)(mU)(fG)(mU)#(fC)#(mA)#(fA)#(mU)#(mC)#(mA)#(fU)	(mU)#(mG)#(fA)(mC)(fA)(mA)(fA)(mU)(fA)(mC)(mG)(mA)(fU)#(mU)#(mA)-DIO

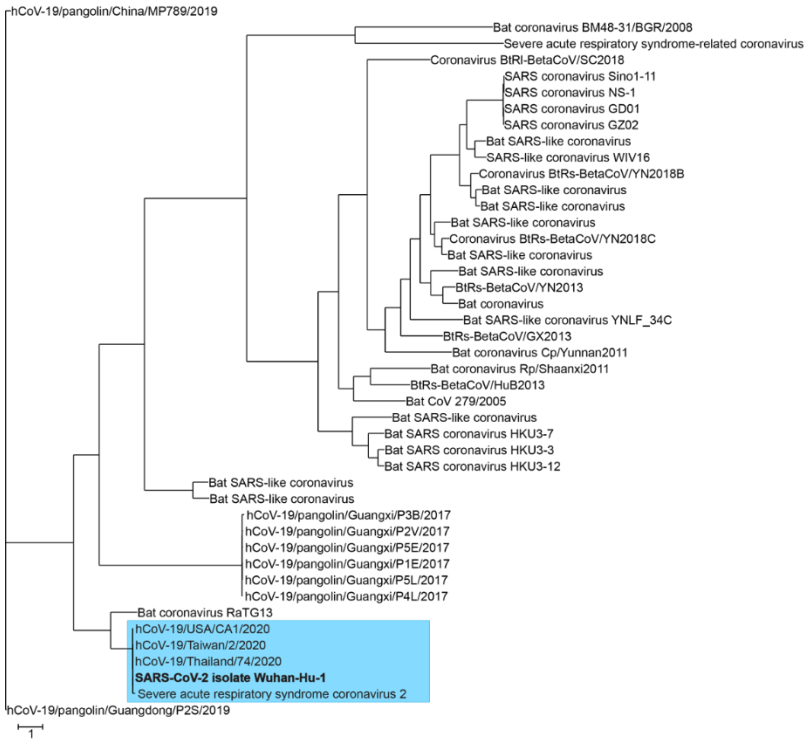

Supporting Fig. 1 | SARS-CoV-2 Family Homology. A maximum-likelihood phylogenetic tree of SARS-CoV-2 and coronaviruses most closely related to SARS-CoV-2 were generated with Augur Tree. Genomic sequences were aligned to five representative SARS-CoV-2 genomes from infected patient isolates (blue box; bold, The SARS-CoV-2 Wuhan-Hu-1 target genomic transcript). Scale bar for branch length indicates substitutions per site.

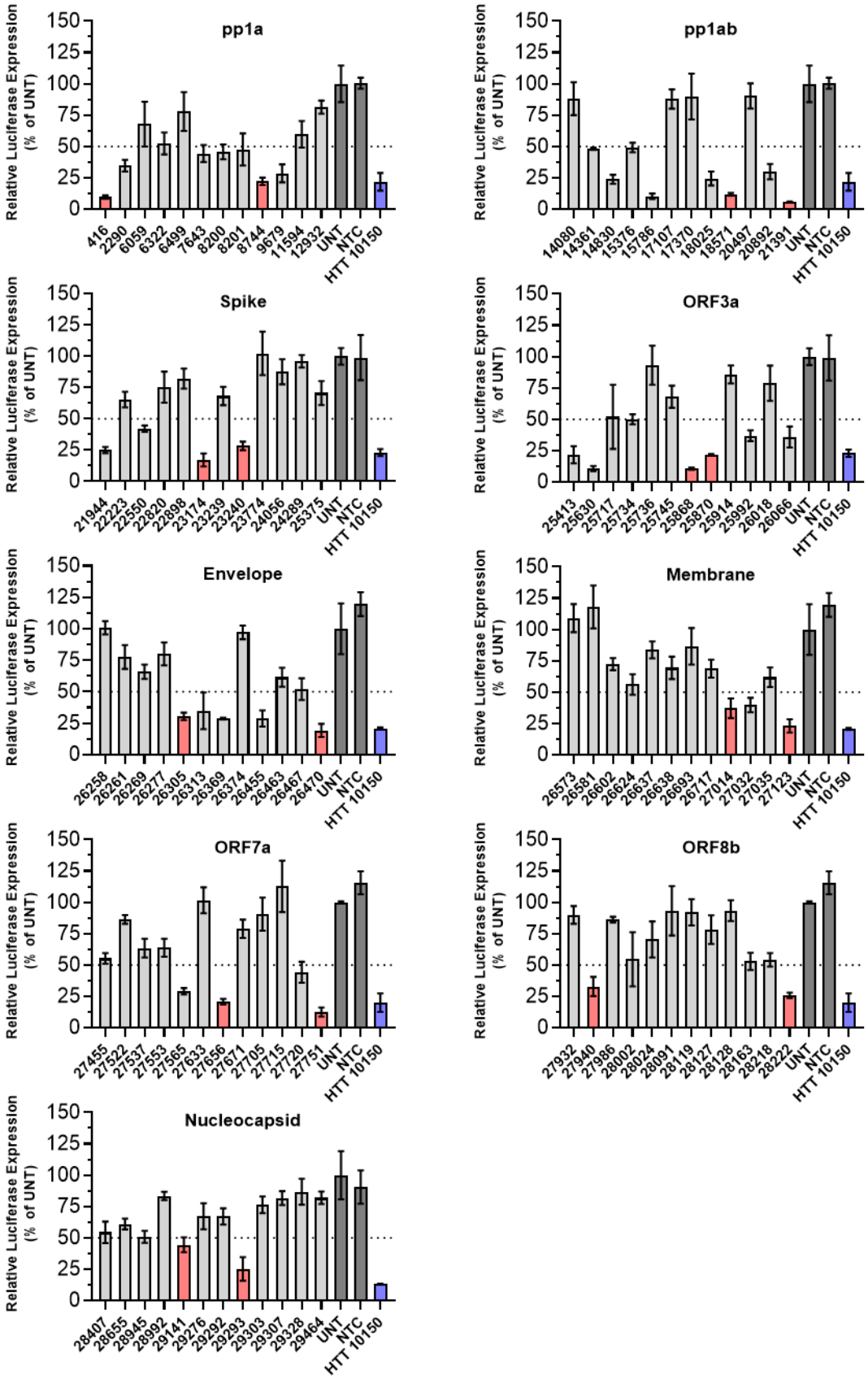
pp1a
Relative Luciferase Expression (% of UNT)
150
125
100
75
50
25
0
416
2290
6059
6322
6499
7643
8200
8201
8744
9679
11594
12932
UNT
NTC
HTT 10150
pp1ab
14080
14361
14830
15376
15786
17107
17370
18025
18571
20497
20892
21391
UNT
NTC
HTT 10150
Spike
21944
22223
22550
22820
22898
23174
23239
23240
23774
24056
24289
25375
UNT
NTC
HTT 10150
ORF3a
25413
25630
25717
25734
25736
25745
25868
25870
25914
25992
26018
26066
UNT
NTC
HTT 10150
Envelope
26258
26261
26269
26277
26305
26313
26369
26374
26455
26463
26467
26470
UNT
NTC
HTT 10150
Membrane
26573
26581
26602
26624
26637
26638
26693
26717
27014
27032
27035
27123
UNT
NTC
HTT 10150
ORF7a
27455
27522
27537
27553
27565
27633
27656
27671
27705
27715
27720
27751
UNT
NTC
HTT 10150
ORF8b
27932
27940
27986
28002
28024
28091
28119
28127
28128
28163
28218
28222
UNT
NTC
HTT 10150
Nucleocapsid
28407
28655
28945
28992
29141
29276
29292
29293
29303
29307
29328
29464
UNT
NTC
HTT 10150

Supporting Fig. 2 | In Vitro Reporter Assays testing siRNAs for Silencing Activity (matched to Fig. 1e). Percent expression of SARS-CoV-2 reporter in HeLa cells 72 hours after uptake of siRNA (n=3; 1.5 μM). Reporter expressions were assayed using the psiCHECK-2 reporter system targeting 9 genomic regions of SARS-CoV-2. Data presented relative to UNT (mean ± SD of independent biological replicates; top hit: red, UNT/NTC: dark grey, positive control siRNA: blue). Target regions of SARS-CoV-2 are indicated in each graph. The dotted lines indicate 50% silencing. NTC, non-targeting control; UNT, untreated control.

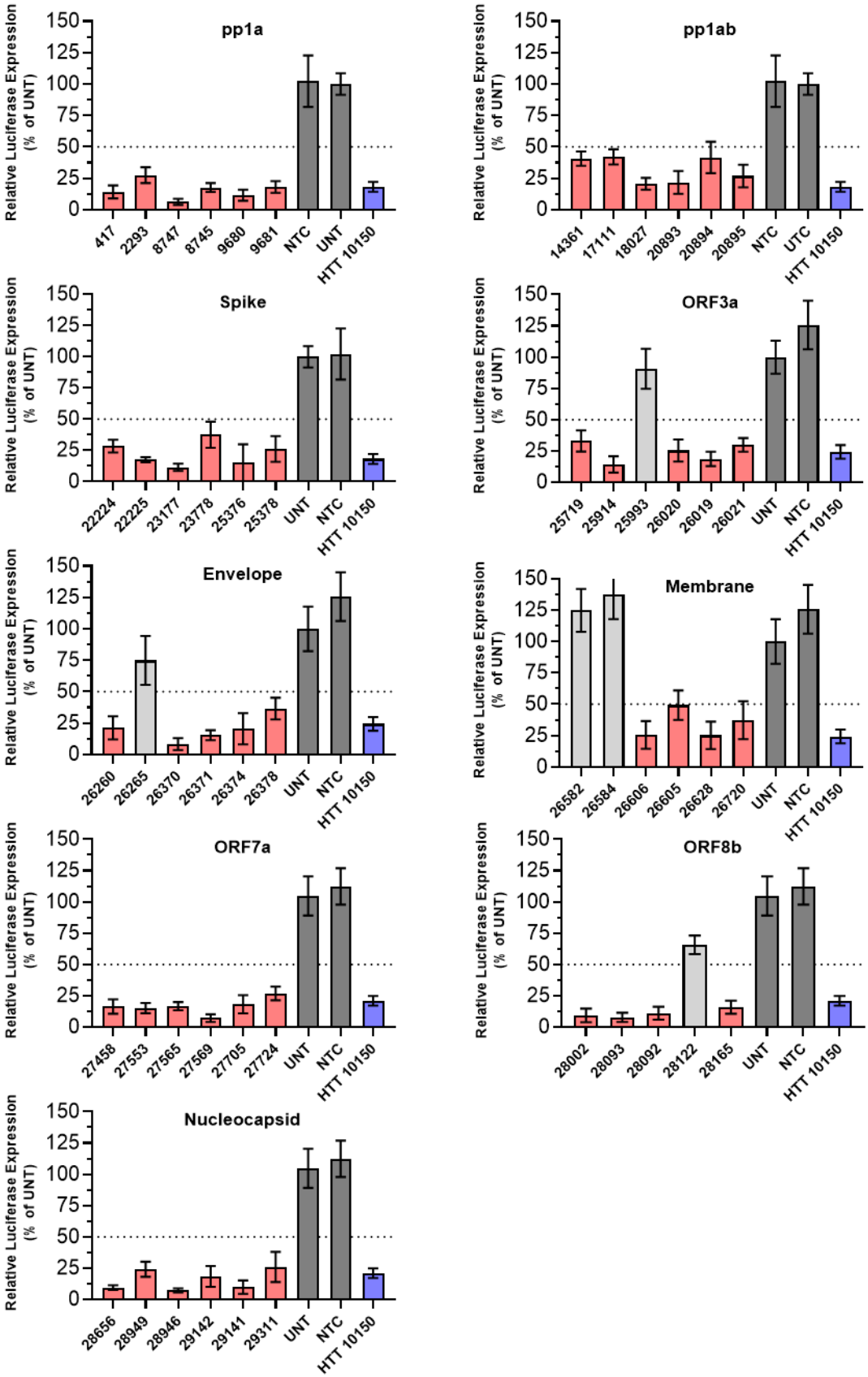
pp1a
Relative Luciferase Expression (% of UNT)
150
125
100
75
50
25
0
417
2293
8747
8745
9680
9681
NTC
UNT
HTT 10150
pp1ab
14361
17111
18027
20893
20894
20895
NTC
UTC
HTT 10150
Spike
22224
22225
23177
23778
25376
25378
UNT
NTC
HTT 10150
ORF3a
25719
25914
25993
26020
26019
26021
UNT
NTC
HTT 10150
Envelope
26260
26265
26370
26371
26374
26378
UNT
NTC
HTT 10150
Membrane
26582
26584
26606
26605
26628
26720
UNT
NTC
HTT 10150
ORF7a
27458
27553
27565
27569
27705
27724
UNT
NTC
HTT 10150
ORF8b
28002
28093
28092
28122
28165
UNT
NTC
HTT 10150
Nucleocapsid
28656
28949
28946
29142
29141
29311
UNT
NTC
HTT 10150

Supporting Fig. 3 | In Vitro Reporter Assays testing ASOs for Silencing Activity. Percent expression of SARS-CoV-2 reporter in HeLa cells 72 hours after uptake of ASO (n=3; 1.5 μM). Reporter expressions were assayed using the psiCHECK-2 reporter system targeting 9 genomic regions of SARS-CoV-2. Data presented relative to UNT (mean ± SD of independent biological replicates; top hit: red, UNT/NTC: dark grey, positive control siRNA: blue). Target regions of SARS-CoV-2 are indicated in each graph. The dotted lines indicate 50% silencing. NTC, non-targeting control; UNT, untreated control.

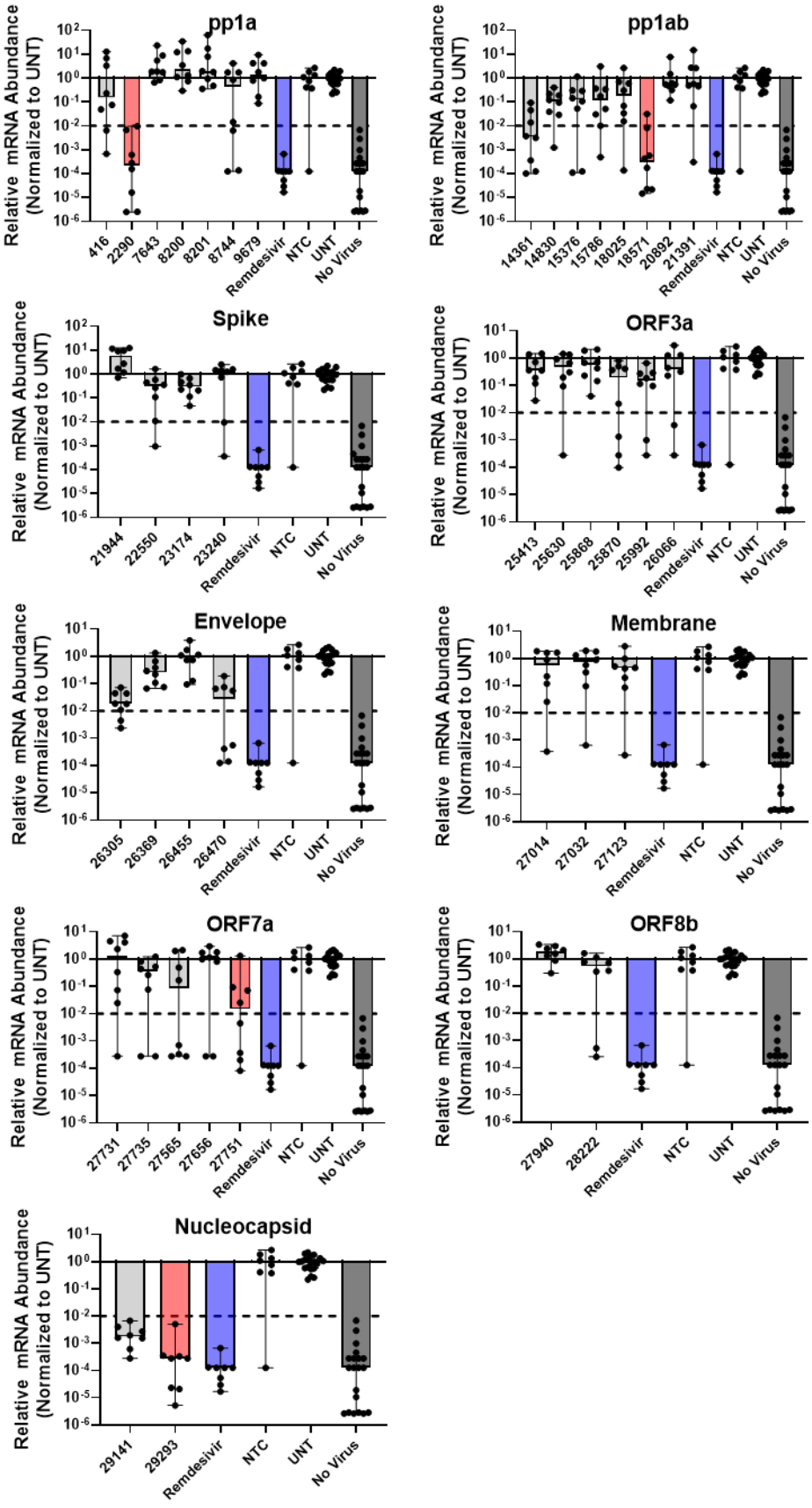
pp1a
Relative mRNA Abundance (Normalized to UNT)
416
2290
7643
8200
8201
8744
9679
Remdesivir
NTC
UNT
No Virus
pp1ab
14361
14830
15376
15786
18025
18571
20892
21391
Remdesivir
NTC
UNT
No Virus
Spike
21944
22550
23174
23240
Remdesivir
NTC
UNT
No Virus
ORF3a
25413
25630
25868
25870
25992
26066
Remdesivir
NTC
UNT
No Virus
Envelope
26305
26369
26455
26470
Remdesivir
NTC
UNT
No Virus
Membrane
27014
27032
27123
Remdesivir
NTC
UNT
No Virus
ORF7a
27731
27735
27565
27656
27751
Remdesivir
NTC
UNT
No Virus
ORF8b
27940
28222
Remdesivir
NTC
UNT
No Virus
Nucleocapsid
29141
29293
Remdesivir
NTC
UNT
No Virus

Supporting Fig. 4 | SARS-CoV-2 infection screen identifies target sites susceptible to RNAi based modulation (matched to Fig. 2a). Relative abundance of viral mRNA in supernatant of $A549^{ACE2/TMPRSS2}$ cells 48 hours post-infection of SARS-CoV-2 with MOI 0.1. siRNAs were transfected 36 hours prior to the infection (siRNA: n=8, controls: n=20; 10 nM). Remdesivir with 5 μM was used as a positive control for antiviral activity. No virus represents cells which were not infected with virus. Abundance of viral mRNA was measured by qRT-PCR. Data presented relative to UNT (median ± 95% CI of independent biological replicates; top hit: red, NTC/UNT/no virus: dark grey, remdesivir: blue). Dotted line indicates 99% reduction in mRNA abundance. MOI, multiplicity of infection; NTC, non-targeting control; UNT, untreated control.

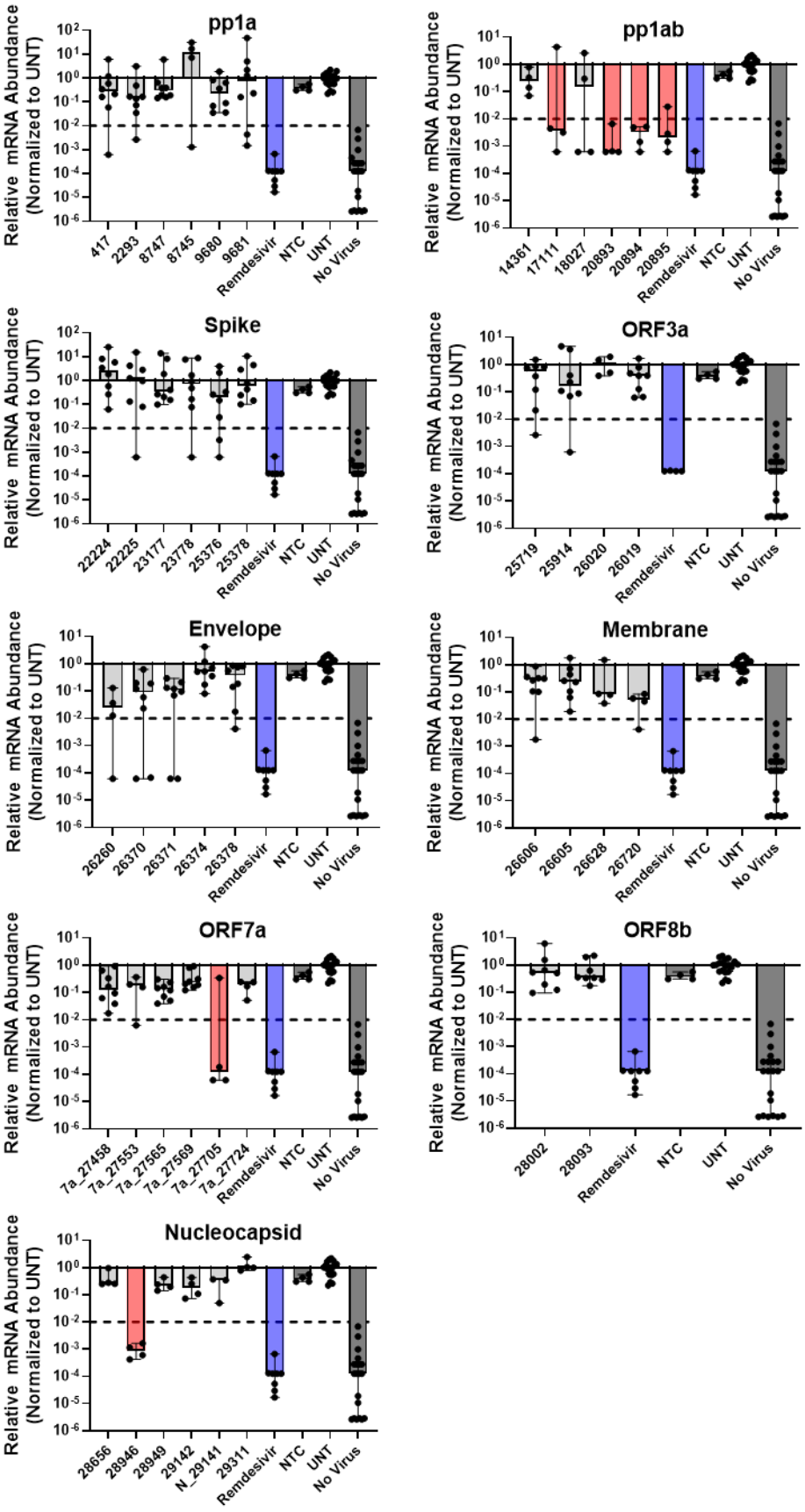
pp1a
Relative mRNA Abundance (Normalized to UNT)
417
2293
8747
8745
9680
9681
Remdesivir
NTC
UNT
No Virus
pp1ab
14361
17111
18027
20893
20894
20895
Remdesivir
NTC
UNT
No Virus
Spike
22224
22225
23177
23778
25376
25378
Remdesivir
NTC
UNT
No Virus
ORF3a
25719
25914
26020
26019
Remdesivir
NTC
UNT
No Virus
Envelope
26260
26370
26371
26374
26378
Remdesivir
NTC
UNT
No Virus
Membrane
26606
26605
26628
26720
Remdesivir
NTC
UNT
No Virus
ORF7a
7a_27458
7a_27553
7a_27565
7a_27569
7a_27705
7a_27724
Remdesivir
NTC
UNT
No Virus
ORF8b
28002
28093
Remdesivir
NTC
UNT
No Virus
Nucleocapsid
28656
28946
28949
29142
N_29141
29311
Remdesivir
NTC
UNT
No Virus

Supporting Fig. 5 | SARS-CoV-2 infection screen identifies target sites susceptible to ASO based modulation. Relative abundance of viral mRNA in supernatant of $A549^{ACE2/TMPRSS2}$ cells 48 h post-infection of SARS-CoV-2 with MOI 0.1. ASOs were transfected 36 hours prior to the infection (ASO: n=8, controls: n=20; 25 nM). Remdesivir with 5 µM was used as a positive control for antiviral activity. No virus represents cells which were not infected with virus. Abundance of viral mRNA was measured by qRT-PCR. Data presented relative to UNT (median ± 95% CI of independent biological replicates; top hit: red, NTC/UNT/no virus: dark grey, remdesivir: blue). Dotted line indicates 99% reduction in mRNA abundance. MOI, multiplicity of infection; NTC, non-targeting control; UNT, untreated control.

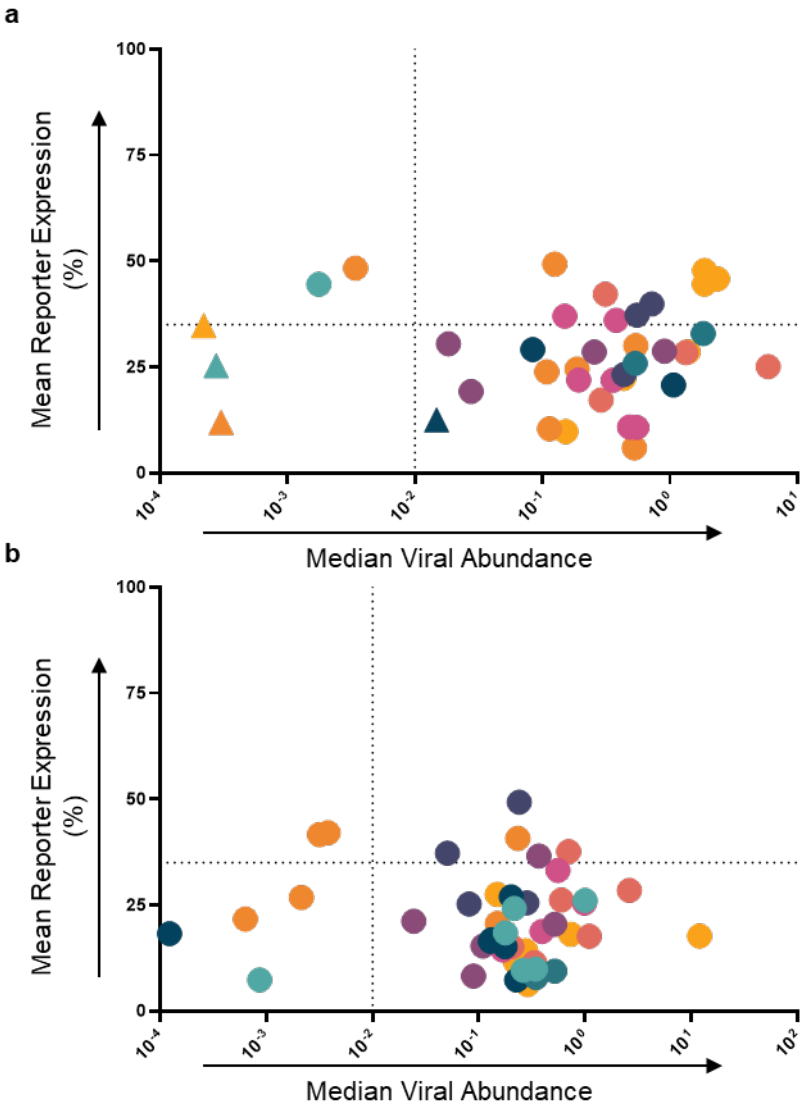

Supporting Fig. 6 | Reporter assay hits do not correlate with activity against live virus. Screening results from the reporter assay are plotted against the results of the SARS-CoV-2 infection model for siRNAs (a) and ASOs (b). Mean reporter expression was obtained data from **Supporting Figure 2 and 3** for siRNAs and ASOs, respectively. Median viral abundance was obtained data from **Supporting Figure 4 and 5** for siRNAs and ASOs, respectively. Triangles indicate the lead siRNAs selected in screening. Dotted lines indicate 35% silencing in reporter expression and 99% reduction in viral abundance.

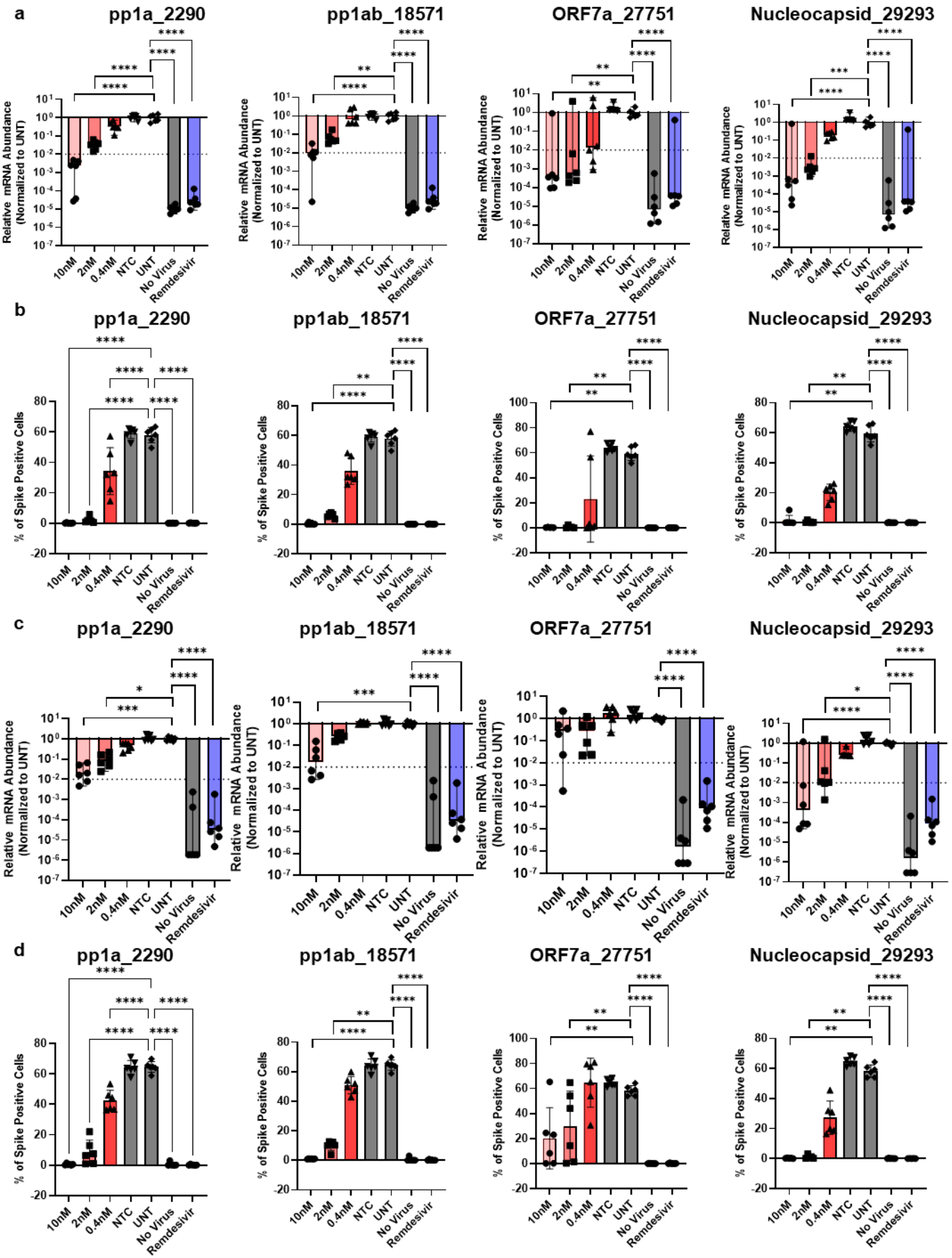
a
pp1a_2290
pp1ab_18571
ORF7a_27751
Nucleocapsid_29293
Relative mRNA Abundance (Normalized to UNT)
b
% of Spike Positive Cells
c
d
10nM
2nM
0.4nM
NTC
UNT
No Virus
Remdesivir

Supporting Fig. 7 | Lead siRNA potently block SARS-CoV-2 infection (matched to Fig. 2b,c). Samples collected and analyzed from $A549^{ACE2plus}$ cells 48 hours post-infection of SARS-CoV-2 with MOI 0.1 (a,b) or 0.4 (c,d). siRNAs were transfected 36 hours prior to the infection (n=6; concentration indicated). Remdesivir with 5 μM was used as a positive control for antiviral activity. No virus represents cells which were not infected with virus. **a,c,** Abundance of viral mRNA was measured by qRT-PCR. Data presented relative to UNT (median ± 95% CI of independent biological replicates; NTC/UNT/no virus: dark grey, remdesivir: blue). Dotted line indicates 99% reduction in mRNA abundance. **b,d,** Percent of spike protein positive cells were determined by immunofluorescence staining (mean ± SD of independent biological replicates; NTC/UNT/no virus: dark grey, remdesivir: blue). One-way ANOVA with Dunnett test for multiple comparisons (****P < 0.0001, ***P < 0.001, **P < 0.01, *P < 0.05). MOI, multiplicity of infection; NTC, non-targeting control; UNT, untreated control.

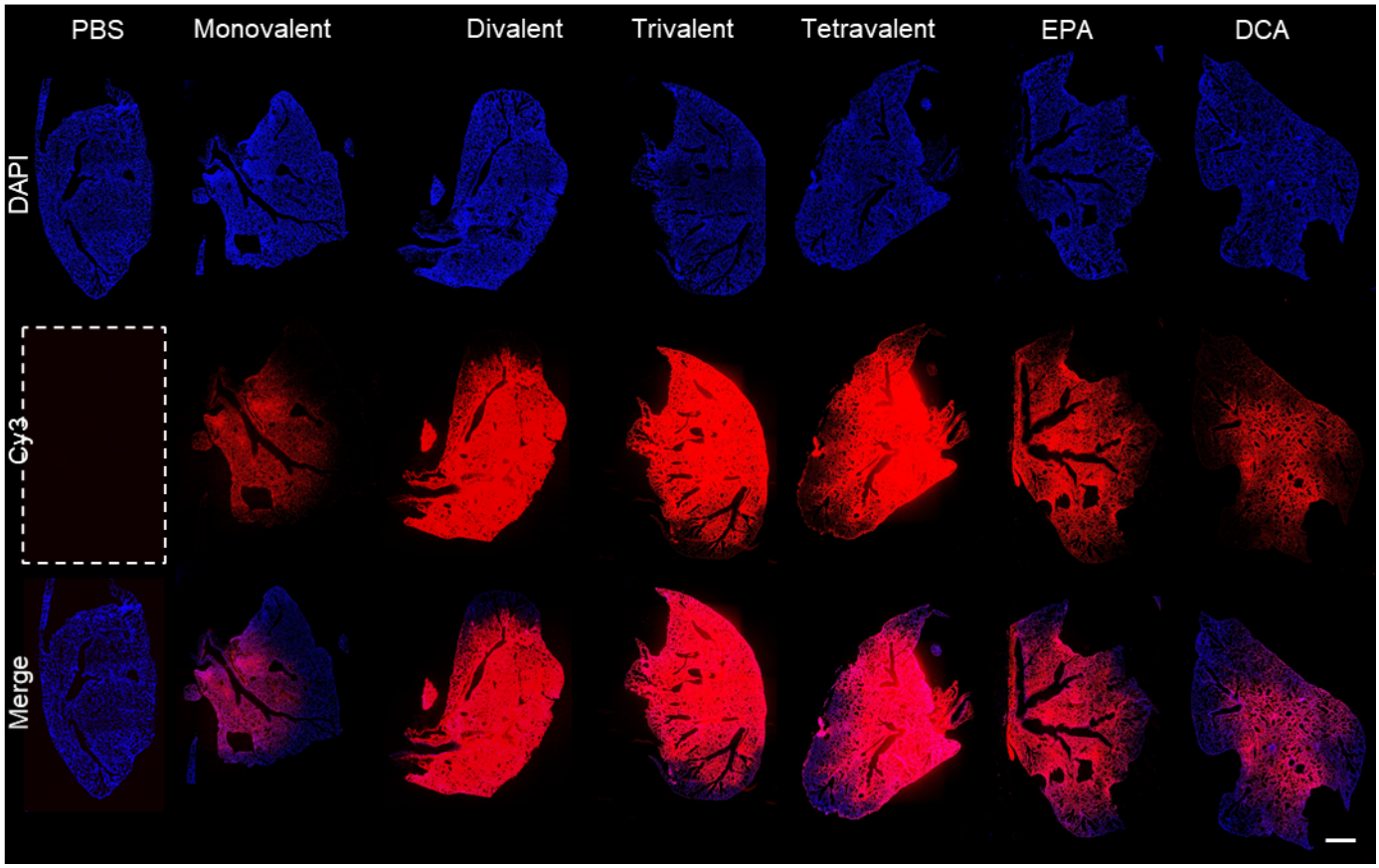

Supporting Fig. 8 | Single channel images of Figure 3c (top). Distribution of siRNA (Cy3, red) with staining of DAPI (blue). Original magnification, ×5. Scale bar: 1 mm.

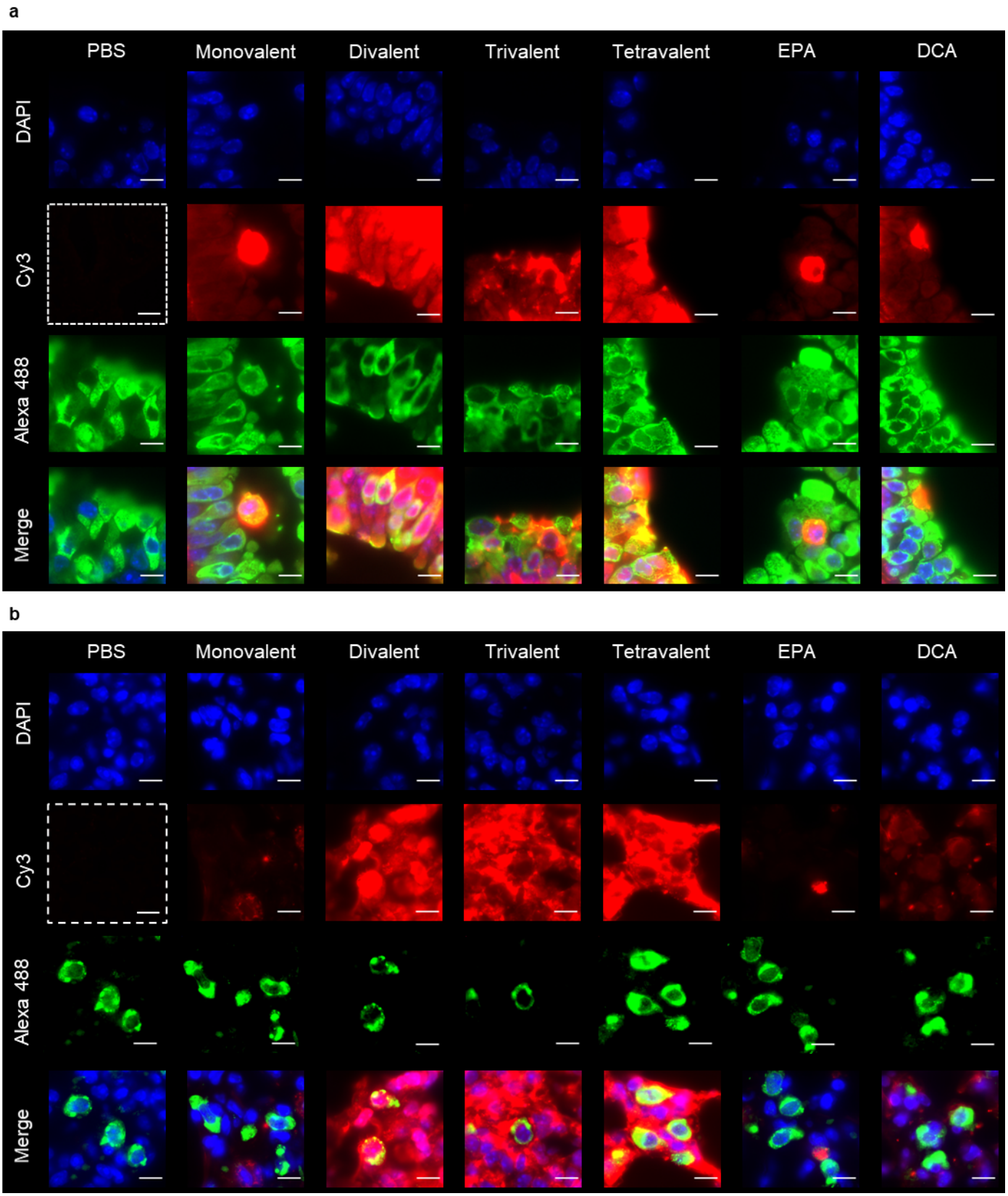
a
PBS
Monovalent
Divalent
Trivalent
Tetravalent
EPA
DCA
DAPI
Cy3
Alexa 488
Merge
b
PBS
Monovalent
Divalent
Trivalent
Tetravalent
EPA
DCA
DAPI
Cy3
Alexa 488
Merge

Supporting Fig. 9 | Single channel images of Figure 3c (middle and bottom). a, distribution of siRNA (Cy3, red) with staining of club cells (AlexaFluor 488, green), and DAPI (blue). **b,** Distribution of siRNA (Cy3, red) with staining of type II alveoli (AlexaFluor 488, green), and DAPI (blue). Original magnification, ×40. Scale bar: 10 μm.

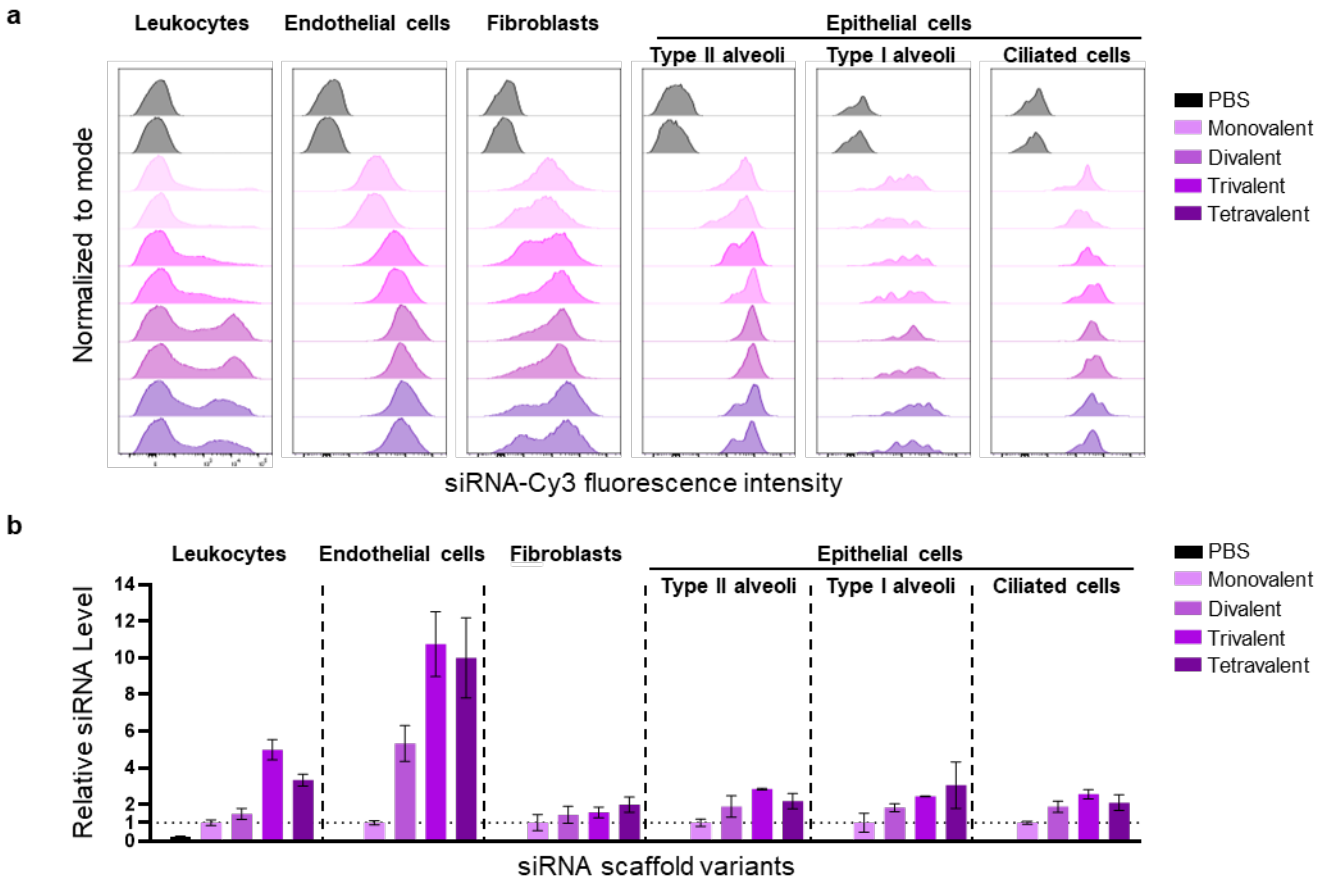

Supporting Fig. 10| Local administration of multivalent fully chemically modified siRNA supports improved accumulation in different lung cell populations. siRNA uptake in leukocytes ($CD45^{+}$), endothelial cells ($CD45^{-}CD31^{+}CD326^{-}$), fibroblasts ($CD45^{-}CD31^{-}CD326^{-}CD140a^{+}$), type II alveoli ($CD45^{-}CD31^{-}CD326^{med}MHCII^{+}$), type I alveoli ($CD45^{-}CD31^{-}CD326^{low}MHCII^{-}$), and ciliated cells ($CD45^{-}CD31^{-}CD326^{hi}MHCII^{-}$) after intratracheal injection of siRNA in mice sacrificed at 24 hours measured from flow cytometry analysis (n=2 mice; 3.75 mg/kg). **a,** Histograms presented Cy3 labeled siRNA fluorescence intensity. Each histogram represents independent biological replicates. **b,** Geometric mean fluorescence intensity presented relative to monovalent siRNA of each cell population (mean ± SD of independent biological replicates).

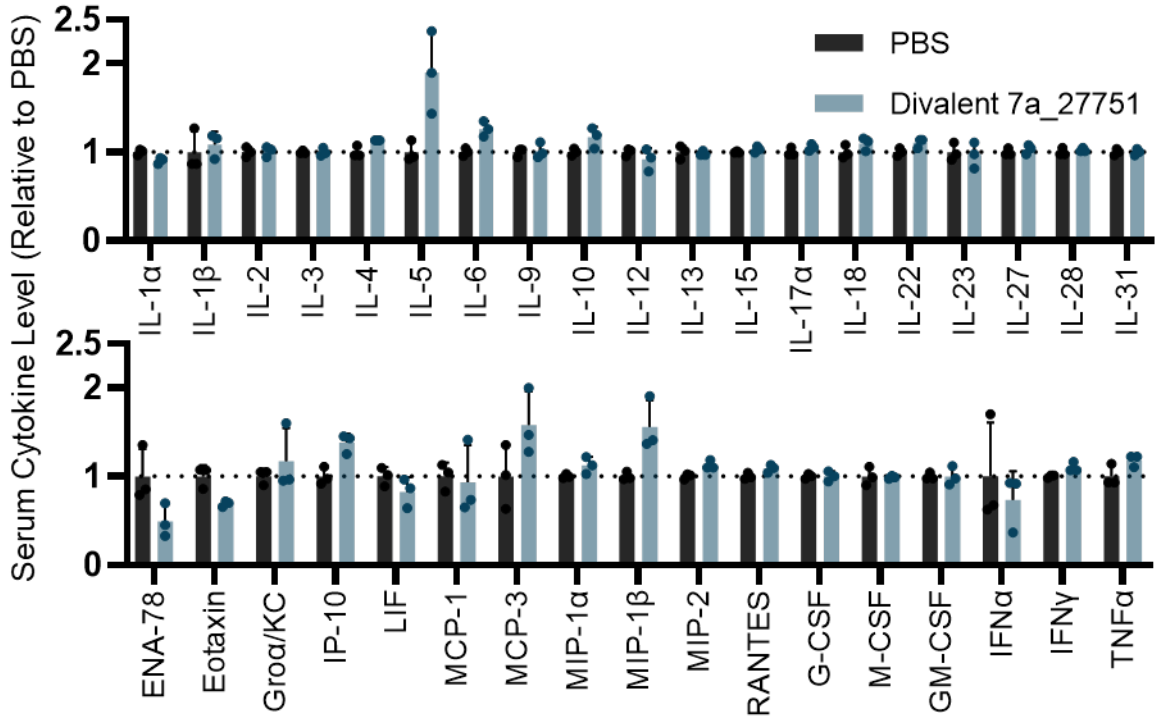

Supporting Fig. 11 | Local administration of high dose divalent fully chemically modified siRNA does not induce serum a cytokine response. Serum cytokine levels 24 hours after intratracheal injection of high dose lead divalent siRNA (n=3 mice; 50 mg/kg). Data presented relative to PBS (mean ± SD of independent biological replicates). One-way ANOVA with Dunnett test for multiple comparisons (***P < 0.001). Dotted lines indicate basal level. EPA, eicosapentaenoic acid; DCA, docosanoic acid; NTC, non-targeting control.

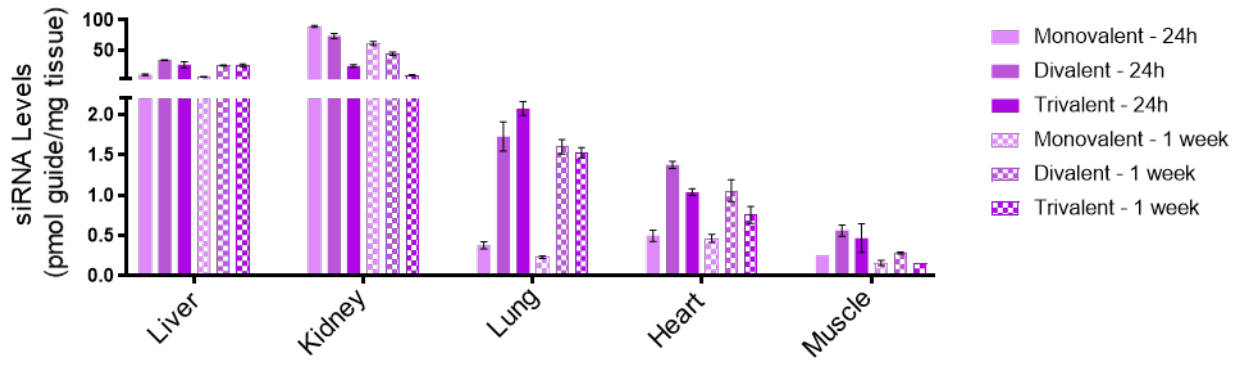

Supporting Fig. 12 | Systemic administration of multivalent fully chemically modified siRNA supports improved lung accumulation. Tissue siRNA levels after subcutaneous injection of siRNA in mice sacrificed at 24 hours (filled) and 1 week (checkered) post-injection measured by PNA hybridization assay (n=2 mice; 20 mg/kg; mean ± SD of independent biological replicates).

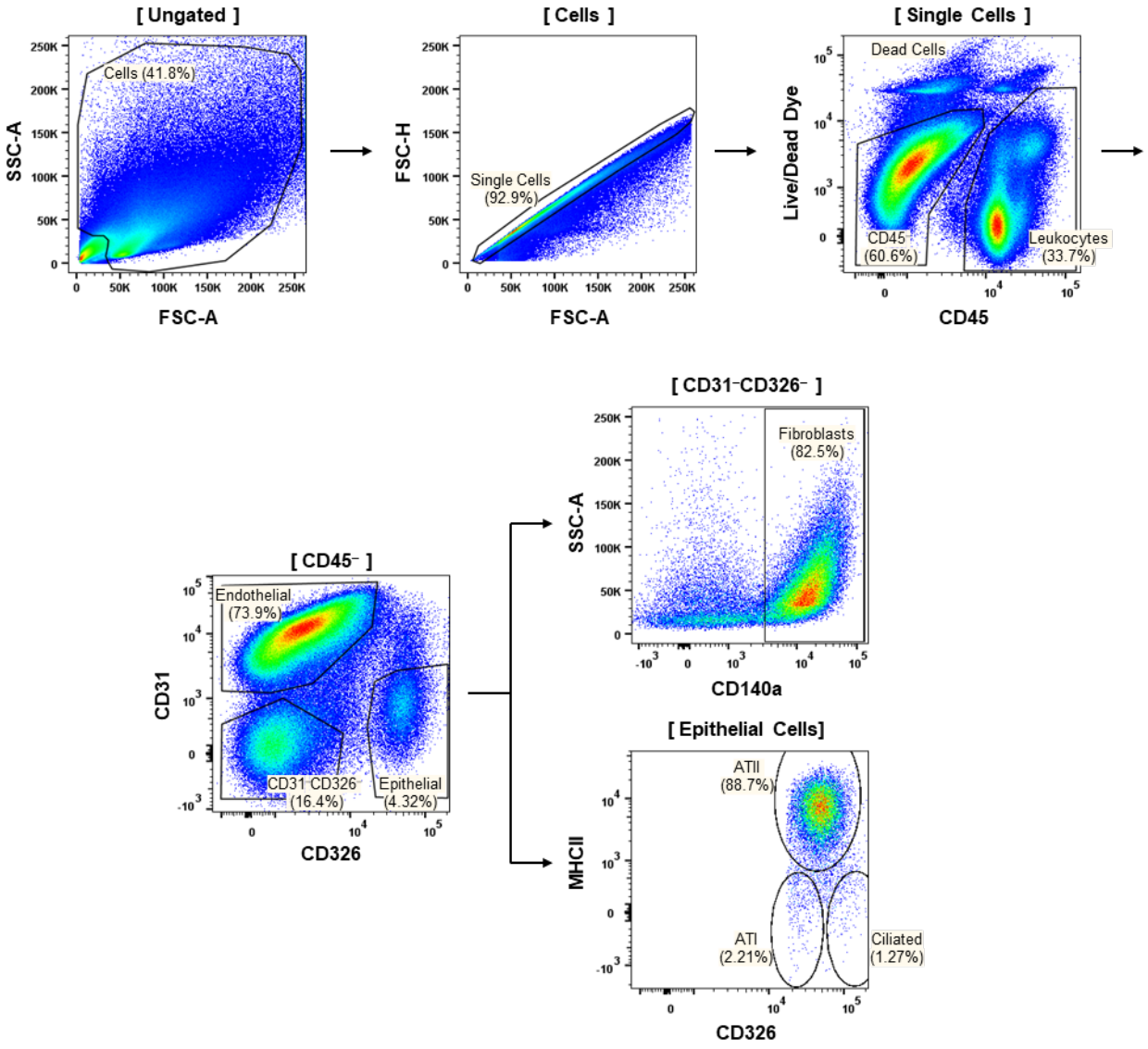

Supporting Fig. 13 | Flow cytometry gating. Debris and non-single cells were excluded by gating on FSC-A×SSC-A and FSC-A×FSC-H. The cell population of different cell types was separated as follows: leukocytes ($CD45^+$), endothelial cells ($CD45^-CD31^+CD326^-$), fibroblasts ($CD45^-CD31^-CD326^-CD140a^+$), epithelial cells ($CD45^-CD31^-CD326^+$), type II alveoli ($CD45^-CD31^-CD326^{med}MHCII^+$), type I alveoli ($CD45^-CD31^-CD326^{low}MHCII^-$), and ciliated cells ($CD45^-CD31^-CD326^{hi}MHCII^-$). A percentage of each cell population to the parent population was presented.